Department of Electrical Engineering and Automation

Safe Navigation for Unmanned Ground Vehicles: Novel Methods for Terrain Traversability Analysis and Human Detection

Juhana Ahtiainen

Aalto University

DOCTORAL DISSERTATIONS

Aalto University publication series
DOCTORAL DISSERTATIONS 175/2017

Safe Navigation for Unmanned Ground Vehicles: Novel Methods for Terrain Traversability Analysis and Human Detection

Juhana Ahtiainen

A doctoral dissertation completed for the degree of Doctor of Science (Technology) to be defended, with the permission of the Aalto University School of Electrical Engineering, at a public examination held at the lecture hall AS1 of the school on 6 October 2017 at 12 o'clock.

Aalto University
School of Electrical Engineering
Department of Electrical Engineering and Automation

Supervising professor
Professor Arto Visala, Aalto University, Finland

Thesis advisors
Professor Emeritus Aarne Halme, Aalto University, Finland
Dr. Jari Saarinen, GIM Oy, Finland

Preliminary examiners
Professor Giovanni Indiveri, University of Salento, Italy
Professor George Nikolakopoulos, Luleå University of Technology, Sweden

Opponent
Professor Marco Hutter, ETH Zürich, Switzerland

Aalto University publication series
DOCTORAL DISSERTATIONS 175/2017

ISBN 978-952-60-7613-3 (printed)
ISBN 978-952-60-7612-6 (pdf)
ISSN-L 1799-4934
ISSN 1799-4934 (printed)
ISSN 1799-4942 (pdf)
http://urn.fi/URN:ISBN:978-952-60-7612-6

Unigrafia Oy
Helsinki 2017

Finland

441 697
Printed matter

Author
Juhana Ahtiainen

Name of the doctoral dissertation
Safe Navigation for Unmanned Ground Vehicles: Novel Methods for Terrain Traversability Analysis and Human Detection

Publisher School of Electrical Engineering

Unit Department of Electrical Engineering and Automation

Series Aalto University publication series DOCTORAL DISSERTATIONS 175/2017

Field of research Automation, Systems and Control Engineering

Manuscript submitted 8 September 2017 **Date of the defence** 6 October 2017

Permission to publish granted (date) 27 April 2017 **Language** English

☐ **Monograph** ☒ **Article dissertation** ☐ **Essay dissertation**

Abstract

Unmanned ground vehicles (UGV) have emerged from research institutes into the outside world over the last decade. For example, UGVs are already part of everyday operations in some mines and harbors around the world. Furthermore, self-driving cars have recently been widely discussed in the news and are expected to be on the market within the next five to ten years. Nonetheless, these UGVs are designed to operate in structured environments and cannot negotiate off-road terrain. Moreover, the reliability of state-of-the-art human detection systems is still not good enough to ensure safety at all times in some application areas.

This thesis proposes novel methods that address these limitations of current UGV systems. It presents the whole chain of developing a UGV system for off-road environments, but the main result of the thesis is to describe the novel terrain traversability analysis methods developed for unstructured environments. It also presents a new, efficient representation of traverasbility mapping and proposes two new approaches for traversability classification that exploit this representation. Furthermore, it presents two innovative methods for augmenting traversability with ultra-wideband (UWB) radar data. Since UWB radars can penetrate some amount of vegetation, the developed methods enable the clearance of obstacle-free vegetation (an area of vegetation that could be driven through) from the generated traversability maps, which is not possible with current state-of-the-art methods.

The thesis also presents two novel human detection methods that exploit 2D LIDAR (Light Detection and Ranging) and radar data, respectively. The LIDAR-based human detection method is computationally very efficient, whereas the radar-based method (utilizing only radar data) demonstrates the potential of radar sensors, typically more robust against adverse weather conditions, in human detection applications. The developed methods provide valuable insights into exploiting additional sensor modalities to supplement traditionally used, camera-based human detection methods.

The performance of all the developed methods was evaluated by conducting extensive field experiments using real UGV systems. The results demonstrate that the methods proposed in this thesis enable safe navigation performance for UGVs, even in densely vegetated, populated environments.

Keywords traversability estimation, obstacle detection, human detection, ultra-wideband radar, unmanned ground vehicle

ISBN (printed) 978-952-60-7613-3 **ISBN (pdf)** 978-952-60-7612-6

ISSN-L 1799-4934 **ISSN (printed)** 1799-4934 **ISSN (pdf)** 1799-4942

Location of publisher Helsinki **Location of printing** Helsinki **Year** 2017

Pages 210 **urn** http://urn.fi/URN:ISBN:978-952-60-7612-6

Aalto-yliopisto

Tiivistelmä

Aalto-yliopisto, PL 11000, 00076 Aalto www.aalto.fi

Tekijä
Juhana Ahtiainen

Väitöskirjan nimi
Miehittämättömien ajoneuvojen turvallinen navigointi: uusia menetelmiä kulkukelpoisuuden analysointiin ja ihmisten havainnointiin

Julkaisija Sähkötekniikan korkeakoulu

Yksikkö Sähkötekniikan ja automaation laitos

Sarja Aalto University publication series DOCTORAL DISSERTATIONS 175/2017

Tutkimusala Automaatio, systeemit ja säätötekniikka

Käsikirjoituksen pvm 08.09.2017 **Väitöspäivä** 06.10.2017

Julkaisuluvan myöntämispäivä 27.04.2017 **Kieli** Englanti

☐ **Monografia** ☒ **Artikkeliväitöskirja** ☐ **Esseeväitöskirja**

Tiivistelmä

Miehittämättömät ajoneuvot (Unmanned Ground Vehicle, UGV) ovat viime vuosikymmenen aikana vähitellen siirtyneet tutkimuslaboratorioista osaksi jokapäiväistä elämäämme. Esimerkiksi monissa kaivoksissa ja satamissa on nykyisin tuotantokäytössä ilman kuljettajaa liikkuvia ajoneuvoja. Autonomiset autot ovat viime aikoina olleet runsaasti esillä tiedotusvälineissä. Niiden uskotaan tulevan markkinoille jo seuraavan viiden vuoden aikana. Edellä esimerkkeinä mainitut miehittämättömät ajoneuvot on kuitenkin kehitetty toimimaan strukturoidussa ympäristössä. Ne eivät pysty operoimaan ennalta tuntemattomassa kompleksisessa maastossa. Miehittämättömien ajoneuvojen havainnointijärjestelmien luotettavuus ei myöskään vielä ole kaikkiin sovelluksiin riittävän hyvä ihmisten turvallisuuden takaamiseksi.

Tässä väitöskirjassa esitellään uusia menetelmiä vastaamaan edellä mainittuihin UGV-järjestelmien haasteisiin. Työssä kuvaillaan UGV-järjestelmän koko kehitysprosessi, mutta tärkeimmät tulokset ovat uudet maaston kulkukelpoisuuden estimointimenetelmät, joilla mahdollistetaan turvallinen navigointi myös monimuotoisessa kasvillisuuden peittämässä maastossa. Työssä esitetään uusi kolmiulotteinen ympäristökuvaus kulkukelpoisuuskartoitukseen. Tällä mahdollistetaan tehokas kulkukelpoisuuden estimointi. Lisäksi esitellään kaksi innovatiivista menetelmää ultralaajakaistatutkan (UWB) mittausten yhdistämiseksi UGV:n ympäristömalliin. Näin mahdollistetaan läpiajettavan kasvillisuuden oikea luokittelu.

Työssä esitellään myös kaksi uutta menetelmää ihmisten havainnointiin. Niissä hyödynnetään laser- ja tutkamittauksia kamerapohjoisten menetelmien sijaan. Lasermittauksiin perustuva menetelmä vaatii hyvin vähän laskentatehoa ja soveltuu siksi hyvin myös järjestelmiin, joissa laskentateho on rajoittava tekijä. Tutkamittauksia hyödyntävä menetelmä mahdollistaa mittaukset myös vaikeissa sääoloissa. Kehitetyt menetelmät eivät yksinään ole riittävän luotettavia kaikkien ihmisten havaitsemiseen, mutta ne tarjoavat arvokasta lisätietoa yhdistettäväksi perinteisillä kamerapohjaisilla menetelmillä saatujen havaintojen kanssa.

Kaikkien tässä työssä kehitettyjen menetelmien suorituskykyä arvioitiin laajamittaisilla kenttätesteillä aitoja UGV-järjestelmiä käyttäen. Tulokset osoittavat, että näiden menetelmien avulla on mahdollista kehittää miehittämätön ajoneuvo, joka pystyy havaitsemaan ihmiset ja muut esteet myös tiheän kasvillisuuden seassa.

Avainsanat kulkukelpoisuuden estimointi, esteiden havainnointi, ihmisen havainnointi, laajakaista-tutka, miehittämätön ajoneuvo

ISBN (painettu) 978-952-60-7613-3 **ISBN (pdf)** 978-952-60-7612-6

ISSN-L 1799-4934 **ISSN (painettu)** 1799-4934 **ISSN (pdf)** 1799-4942

Julkaisupaikka Helsinki **Painopaikka** Helsinki **Vuosi** 2017

Sivumäärä 210 **urn** http://urn.fi/URN:ISBN:978-952-60-7612-6

Preface

This research was conducted in the Centre of Excellence in Generic Intelligent Machines (CoE-GIM) at Aalto University, excluding my six-month research visit to Australian Centre for Field Robotics and the last few years of occasional writing in the corner of our living room or in the nearby library. My research was mainly project-driven and, therefore, funded by many organizations through different research projects. I would, thus, like to gratefully acknowledge the support from Finnish Defence Forces, TEKES (Finnish Funding Agency for Technology and Innovation), FIMA (Forum of Intelligent Machines ry), Academy of Finland, and Finnish Metals and Engineering Competence Cluster (FIMECC). Furthermore, I greatly appreciate the personal grants from Finnish Society of Automation, and Henry Fordin Säätiö that enabled me to travel to several conferences to present my research and finalize this thesis while no longer employed at the university.

This thesis was eventually completed with the support of many people. Although they are too numerous to name here individually, I am grateful for all the help and friendship of all these people during these years. Nonetheless, I would like to acknowledge some individuals personally.

I am grateful to Professor Emeritus Aarne Halme, leader of CoE-GIM and my supervisor for the greater part of my thesis work, for his valuable advice during these years. Your input was indispensable, particularly towards the end of this project. I would also like to thank Professor Arto Visala for taking over as my official supervisor and convincing me to finalize this project. Furthermore, I am much obliged to Professor Pekka Appelqvist for recruiting me in the first place and for his advice while my instructor at early stages of my thesis work.

Huge thanks to Dr. Jari Saarinen — my instructor for most of the thesis work — for his valuable advice during these years, for motivating me,

and for making things happen. Big thanks also to Dr. Thierry Peynot for instructing me during my Australian exchange and for successful cooperation afterwards, as well as to Dr. Jussi Suomela for supervising me for a short period of time and for enabling my research exchange. Moreover, the pre-examiners of this thesis, Professor Giovanni Indiveri and Professor George Nikolakopoulos, have my gratitude for their feedback, which helped me improve this thesis.

Thanks also to all the colleagues and co-workers who helped me along the way. Mr. Jere Knuuttila and Dr. Sami Terho, who shared an office with me, particularly deserve a big thanks for all the advice and excellent discussions. Moreover, I would like to thank Dr. Tapio Taipalus for associating me with his human detection experiments. Furthermore, thanks to Dr. Todor Stoyanov for cooperating with the NDT-related research.

Thanks to all my friends who have kept me more or less sane during these years. Specifically, I would like to thank Dr. Olli Mali and Mr. Lauri Kuuliala for all the good talks, some of which even related to this thesis. Naturally, I want to thank my parents, my sister, and my grandparents for all the support over the years. Most importantly, I want to thank my lovely wife, Ulla, for her patience, love, and understanding, as well as being there when most needed. Lastly, thank you, Otso, for being born. Your smile lights up my world.

Helsinki, August 29, 2017,

Juhana Ahtiainen

Contents

List of Publications

This thesis consists of an overview and of the following publications which are referred to in the text by their Roman numerals.

I Pekka Appelqvist, Jere Knuuttila, and Juhana Ahtiainen. Development of an Unmanned Ground Vehicle for Task-Oriented Operation - Considerations on Teleoperation and Delay. In *IEEE/ASME International Conference on Advanced Intelligent Mechatronics (AIM)*, Zürich, Switzerland, pp. 258:1–258:6., September 2007.

II Pekka Appelqvist, Jere Knuuttila, and Juhana Ahtiainen. Mechatronics Design of an Unmanned Ground Vehicle for Military Applications. *Mechatronic Systems Applications, Annalisa Milella Donato Di Paola and Grazia Cicirelli (Ed.)*, Chapter 15, pp. 237–262, InTech, March 2010.

III Juhana Ahtiainen, Sami Terho, and Sampsa Koponen. Radar based detection and tracking of a walking human. In *IFAC Symposium of Intelligent Autonomous Vehicles (IAV)*, Lecce, Italy, 43/16, pp. 437–442, September 2010.

IV Tapio Taipalus and Juhana Ahtiainen. Human Detection and Tracking with Knee-High Mobile 2D LIDAR. In *IEEE International Conference on Robotics and Biomimetics (ROBIO)*, Karon Beach, Phuket, Thailand, pp. 1672–1677, December 2011.

V Juhana Ahtiainen, Thierry Peynot, Jari Saarinen, and Steven Sched-

ing. Augmenting Traversability Maps with Ultra-Wideband Radar to Enhance Obstacle Detection in Vegetated Environments. In *IEEE/RSJ International Conference on Intelligent Robots and Systems (IROS)*, Tokyo, Japan, pp. 5148–5155, November 2013.

VI Juhana Ahtiainen, Thierry Peynot, Jari Saarinen, Steven Scheding, and Arto Visala. Learned Ultra-Wideband RADAR Sensor Model for Augmented LIDAR-based Traversability Mapping in Vegetated Environments. In *The International Conference on Information Fusion*, Washington, DC, USA, pp. 953–960, July 2015.

VII Juhana Ahtiainen, Todor Stoyanov, and Jari Saarinen. Normal Distributions Transform Traversability Maps: LIDAR-Only Approach for Traversability Mapping in Outdoor Environments. *Journal of Field Robotics*, 34(3):600–621, May 2017.

Author's Contribution

Publication I: "Development of an Unmanned Ground Vehicle for Task-Oriented Operation - Considerations on Teleoperation and Delay"

The author was responsible for instrumentation and implementation of the software related to the UGV control system, as well as partially designing the system and software, along with the telecommunication delay experiment design and execution. The authors jointly wrote the conference paper.

Publication II: "Mechatronics Design of an Unmanned Ground Vehicle for Military Applications"

The author was responsible for mounting the hardware components and implementing the software related to the UGV control system, as well as partially designing the system and software design, along with designing and executing the telecommunication delay experiments. Furthermore, the author integrated the payload, partially contributed to the navigation system's development, and participated in the overall system evaluation. The authors jointly wrote the article.

Publication III: "Radar based detection and tracking of a walking human"

The author was jointly responsible for developing the Doppler radar-based human detection algorithm and fully responsible for the sensor fusion and tracking algorithm. The author jointly wrote the paper with Dr. Sami

Terho, under the guidance of Dr. Sampsa Kosonen.

Publication IV: "Human Detection and Tracking with Knee-High Mobile 2D LIDAR"

The author jointly wrote the conference paper with Dr. Tapio Taipalus. The author was partially responsible for the test design and execution, as well as the proposed method's data analysis and validation.

Publication V: "Augmenting Traversability Maps with Ultra-Wideband Radar to Enhance Obstacle Detection in Vegetated Environments"

The author wrote this article; its contents were solely based on the author's work under the other authors' guidance.

Publication VI: "Learned Ultra-Wideband RADAR Sensor Model for Augmented LIDAR-based Traversability Mapping in Vegetated Environments"

The author wrote this article; its contents were solely based on the author's work under the other authors' guidance.

Publication VII: "Normal Distributions Transform Traversability Maps: LIDAR-Only Approach for Traversability Mapping in Outdoor Environments"

The author wrote this article; its contents were solely based on the author's work under the other authors' guidance.

List of Figures

List of Tables

List of Abbreviations

Abbreviation	Explanation
2D	two-dimensional
3D	three-dimensional
ACTC	augmented constant threshold classifier
AGV	automatic/automated ground vehicle
ALV	autonomous land vehicles
ALVINN	autonomous land vehicle in a neural network
BRAiVE	BRAin-DrIVE
CMU	Carnegie Mellon University
CNN	convolutional neural network
C-SVC	C-support vector classifier
CTC	constant threshold classifier
DARPA	Defence Advanced Research Projects Agency
DEM	digital elevation model
DGC	DARPA Grand Challenge
DSA	Doppler signature analysis
DUC	DARPA Urban Challenge
ELROB	European Land-Robot Trial
ESC	emergency stop circuit
EVC	estimated velocity comparison
FMCW	frequency modulated continuous wave
FN	false negative
FNR	false negative rate
FOV	field of view
FP	false positive
GMM	Gaussian mixture model
GNSS	global navigation satellite system
GP	Gaussian process

GPS	global positioning system
GUI	graphical user interface
HMI	human-machine interface
HSMM	hidden semi-Markov model
IMU	inertial measurement unit
LAGR	Learning Applied to Ground Vehicles
LIDAR	light detection and ranging
LS3	Legged Squad Support Systems
MHT	multi-hypothesis tracking
MRF	Markov random field
MLS	multi-level surface
Navlab	Navigation Laboratory
NBC	nuclear, biological, and chemical
NDT	normal distributions transform
NDT-OM	normal distributions transform occupancy map
NDT-TM	normal distributions transform traversability map
NIR	near-infrared
NN	nearest neighbor
NREC	National Robotics Engineering Center
PCA	principal component analysis
PerceptOR	Perception for Off-Road Robotics
RGB-D	red, green, blue, depth
RI	Robotics Institute
RNN	recursive neural network
RTOS	real-time operating system
RTK	real-time kinematic
SCARF	Supervised Classification Applied to Road Following
SDC	self-driving car
SVM	support vector machine
TN	true negative
TNR	true negative rate
TP	true positive
UGCV	unmanned ground combat vehicle
UGV	unmanned ground vehicle
UPI	UGCV PerceptOR Integration
UWB	ultra-wideband
YARF	Yet Another Road Follower

List of Symbols

Symbol	Explanation
μ_I	The mean intensity of one-dimensional Gaussian intensity distribution
r	Circumference of a bounding box
R	Roughness of an NDT cell
ρ	Permeability of an NDT cell
s	Size of cluster bounding box
st	Straightness of a cluster
Σ_I	The variance of one-dimentional Gaussian intensity distribution
T_m	Traversability map
T_{ma}	Augmented traversability map
τ	Traversability index
θ	Inclination of an NDT cell

List of Definitions

Doppler spectrum analysis (DSA)

A method for analyzing Doppler spectrum for periodicity to classify walking people (Publication III).

Estimated velocity comparison (EVC)

A method for comparing estimated target velocity for average walking speed of a human to gain more evidence about the target class (Publication III).

Human probability

A probability of a human candidate/target to be a human (Publication III, Publication IV).

Obstacle-free foliage

An area of vegetation that could be driven through (Publication V, Publication VI).

Direct teleoperation

Operation of a UGV over a distance without a line-of-sight between the vehicle and the operator such that the operator is a constant part of a real-time control loop.

Self-driving car (SDC)

A car developed for structured environments (i.e., public roads and parking lots) that features autonomous functionalities. For the time being, self-driving cars operating within normal traffic still need an operator on the driver's seat to at least monitor the vehicle performance. Although SDCs typically still have passengers/operator inside the vehicle, they are considered as UGVs in this thesis, since the exploited technology is similar regardless of the number of people in the vehicle.

UGV demonstrator

A UGV developed for task-oriented operations in an off-road environment. Publication I and Publication II describe details of the vehicle and development process.

Ultra-wideband radar (UWB)

Radar sensor transmitting very short pulses across wide range of frequencies. Typically, these radars operate at relatively low frequencies ($1\,GHz - 10\,GHz$) and have a bandwidth greater than $500\,MHz$.

Unmanned ground vehicle (UGV)

A vehicle operating on the ground without an onboard human, excluding vehicles moving along rails or tracks as well as vehicles whose operation requires direct visual feedback.

1. Introduction

This chapter presents the background and motivation behind this thesis as well as this work's objectives and scope. Moreover, it also presents summaries of the articles' contents to highlight the author's main contributions. Finally, this chapter describes the structure of the remainder of this thesis.

1.1 Background and Motivation

Unmanned ground vehicles (UGV) can be defined as vehicles that operate on the ground surface without an on-board human presence. The main motivation for developing UGVs is to eliminate the need for people to perform unattractive tasks that are often characterized by the three Ds: dirty, dangerous, and dull. For example, typically work inside a mine is dirty, potentially dangerous and might also be dull, in the case of repetitive work tasks. UGVs are, therefore, currently making their way into mines as well as other areas of industry. Moreover, utilizing UGVs in industry has great potential for improving the performed tasks' quality and productivity.

The aforementioned definition of UGVs only defines that the operator controlling the vehicle, if one exists, is not on the vehicle itself. It does not specify the type of control that an operator might have over the vehicle at any given time; that is, a completely autonomous car and a radio-controlled car both fit inside this definition. This thesis narrows down the definition and only considers vehicles that either have some level of autonomy or are directly teleoperable. We only consider those modes of control in which the operator is a constant part of a real-time control loop without visual feedback as exhibiting direct teleoperation, excluding applications that have a notable level of autonomy or require constant line

of sight between the vehicle and the operator. Furthermore, this thesis concentrates on vehicles operating outdoors and only considers vehicles not restricted by tracks or rails and that can move in any direction permitted by the vehicle kinematics.

UGVs have been developed for decades inside research laboratories around the world and deployed for simple operations in industry from early on. For example, automatic guided vehicles (AGV), driverless transport systems for horizontal movement of materials, have been utilized inside manufacturing facilities and warehouses since the 1950s (Vis, 2006). However, UGVs have only recently been deployed outside research institutes and factories. Currently, autonomous UGVs are already part of operations in some harbors and mines worldwide, while more autonomous systems are unfolding regularly (Kalmar Global, 2016; Sandvik, 2016). Moreover, self-driving cars are currently being developed with vast resources as Google is currently testing a fleet of self-driving cars around the streets of the USA (Google, 2016), and all the major car manufacturers are adding autonomous features into their vehicles daily. According to the boldest predictions, self-driving cars might be on the market already within few years (Connor, 2015).

Nonetheless, the UGVs in industry have been developed to operate only in very case-specific environments, and they rely on strong assumptions about the environment. Furthermore, these autonomous machines still need to be separated from people with a safety fence for the time being. Similarly, self-driving cars have been developed to operate only in structured environments (i.e., on roads and parking lots) and typically cannot negotiate unstructured off-road environments. Moreover, adverse weather condition still cause problems for self-driving cars (Ackerman, 2014), which require further extensive testing in challenging weather conditions.

All UGVs are very complicated systems containing several subsystems. There are no standardized ways to define these subsystems, and two UGVs developed for different applications might differ significantly in structure. However, all UGVs generally perform similar basic functionalities, and hence have similar subsystems. The biggest UGV-related research challenges currently involve perceiving and understanding the operating environment; that is, gathering sensor data and analyzing the data to form an environment model that enables autonomous decision making.

Two tasks in particular are considered the premier challenges in mobile robotics. First, human detection and tracking is a mandatory task for all UGVs operating in populated environments to ensure the people's safety. However, the accuracy requirements for such systems are high, and there are not yet any commercially available human detection modules in the market fulfilling these requirements. Adverse weather conditions, especially, still cause some concern, and the price of required human detection system might be too high for some applications. Second, modeling and interpreting the environment based on sensor data is still in its infancy when dealing with complex environments. For example, there are currently no generally accepted methods for building a map of an unstructured natural environment and interpreting the map such that it can be deduced whether it is safe to traverse through a particular area. People are particularly good at making such deductions, however, this task is considered challenging even for a human operator, especially when relying only on sensor data transmitted to a remote control station.

These shortcomings are widely acknowledged in the research community, and both tasks have been extensively studied over the last decade. Nonetheless, detecting humans with any kind of sensor system still remains a challenging task due to the wide variety of positions and appearances that humans can assume. Moving sensor systems and adverse weather conditions further complicate the task. People trackers are often integrated into human detection systems to add robustness, since they enable acceptable performance in the presence of occlusions. However, human tracking is also a challenging task on its own, since people's behaviors are often completely unpredictable.

Terrain traversability analysis, another imperative task for autonomous vehicles, also remains a partially unsolved problem, since the environment's complexity increases the difficulty of traversability analysis. That is, deducing a smooth road's traversability, for example, is relatively straightforward and can be performed reliably with the current state-of-the-art methods. However, when operating in an off-road environment, the task of determining terrain traversability remains a challenge for the state-of-the-art methods due to the difficulty of capturing and representing the environment's variability. A naive geometric representation of the environment is usually insufficient for safe navigation, as the perception system can often mistakenly interpret obstacle-free vegetation (an area of vegetation that could be driven through) as an obstacle. In practice,

traversing through sparse vegetation is often possible and may be preferable to avoid executing longer paths. It can even be the only acceptable option for the UGV in cases of densely vegetated environments. An experienced human operator typically can make the right choices on-board the vehicle, but this task becomes much more difficult when operating the UGV from a distance, since generating perfect telepresence — a sensation that the operator is physically present at the remote site (Sheridan, 1992) — is extremely difficult due to the diverse perception information required (e.g., visual, audio, vibratory). That is, transmission delays and the limited amount of information transmitted to the control station significantly complicate the operator's task of evaluating the terrain traversability, although, the extent of required sensory information depends on the difficulty of the task at hand. Moreover, the acceptable amount of transmission delay strongly depends on the nominal frequency of the task (Suomela, 2004).

1.2 Research Questions and Objectives

As the previous section discussed, two premier challenges emerge from field robotics; that is, reliable human detection and tracking as well as terrain traversability analysis and mapping in unstructured environments still remain partly unsolved research challenges.

The main research question being studied in this thesis is how to enable safe off-road navigation for UGVs in unstructured natural environments, for example, on densely vegetated fields and other unstructured areas. We studied the whole chain of developing a UGV, but the main contribution is on developing novel methods for human detection and terrain traversability analysis that enhance the navigation performance in vegetated off-road environments that are achievable with current state-of-the-art methods.

The main objective of this thesis was to develop traversability analysis methods for UGVs operating in vegetated environments. These methods in particular can distinguish obstacle-free vegetation from other obstacles, such that UGVs can operate safely in natural, off-road environments.

The second objective was to develop human detection methods that can be used to complement the traditional camera-based human detection approaches. Since most radar sensors are particularly immune to adverse weather conditions, the use of different radars in human detection

systems was studied. The developed methods are stand-alone methods, that is, able to perform human detection without any additional input data. However, these methods can easily be integrable with other human detection approaches that exploit alternative sensor modalities.

Algorithm development for mobile robotic applications requires a test bed that can gather data and validate the performance of the developed methods. Therefore, the third objective of this thesis was to develop a generic off-road capable UGV that can be operated with variable levels of autonomy and be utilized in versatile, task-oriented operations. This UGV is capable of both direct teleoperation and for autonomous operation in off-road environments; however, developing a UGV system from scratch is a huge task, so this thesis has focused on developing the perception and navigation capabilities.

Reaching the aforementioned objectives would make it possible to also deploy UGVs in unstructured, natural, and populated environments; this could significantly boost the productivity and reduce the work-related accidents of several fields in industry. This thesis will present novel methods addressing these objectives and provide experimental validation for all the developed methods. The proposed methods have been implemented on several separate platforms; therefore, this thesis does not present experiments with a UGV running all the proposed algorithms at once. However, all the developed methods have been validated using real UGV systems.

1.3 Summary of the Publications

This doctoral thesis is an article dissertation comprising a summary and seven individual publications. One publication is a journal article, one is a book chapter, and five articles are conference publications. The publications have been numbered in ascending, chronological order and can be divided into three separate groups. The first group (Publication I and Publication II) concentrates on the design aspects involved in developing UGVs, whereas the second group (Publication III and Publication IV) concentrates on human detection methods. The third group (Publication V, Publication VI, and Publication VII) deals with environment modeling and traversability analysis in unstructured natural environments.

Publication I describes the development of a directly teleoperated UGV for task-oriented operation. The vehicle instrumentation is described

in detail, while the main contribution of the publication is not only to identify the different sources of communication delay in teleoperation but also analyze these sources and the effects of the delay.

Publication II provides detailed descriptions about the design and development of a UGV capable of teleoperated, semi-autonomous, and autonomous operation in off-road environments. The article proposes a natural subsystem structure for UGV systems and graphically describes the functions and contents of these subsystems, including a detailed presentation of the involved hardware and software modules. Furthermore, the article describes the performed milestone demonstrations and field tests and discusses the lessons learned from these demonstrations. The article additionally presents and analyzes results from the user interface usability tests that indicated the need for more versatile human-machine interaction, including an option for automatic obstacle detection and traversability analysis.

Publication III proposes a radar-based detection and tracking method for walking humans utilizing two different radar sensors: a frequency modulated continuous wave (FMCW) radar and a Doppler radar. The motion a walking human's different body parts generates a distinguishable Doppler signature that can be detected by analyzing the Doppler spectrum. The FMCW radar data are utilized to track the targets and a Doppler radar is used to analyze the Doppler spectrum, which provides additional information about the classes of the targets. Classifying targets as humans is based on analyzing targets' Doppler spectrum, as well as the targets' speed gained through the tracking process. The proposed method demonstrates that classifying and tracking walking humans is possible using only radar technology, which is more robust against adverse weather conditions than other commonly utilized sensor modalities.

Publication IV presents computationally light human detection method using only a 2D LIDAR. The utilized 2D LIDAR is installed at knee height; the proposed algorithm is based on leg tracker, which detects legs according to a predefined feature list. A human candidate is formed if two legs are sufficiently close to each other, after which the human is tracked using the leg images. The human probability of each tracked target is evaluated based on the predefined features after each new measurement. The proposed method is computationally very light and can be utilized in applications with limited computational capacity.

Publication V addresses the problem of traversing in densely vegetated environments and proposes an innovative method that combines ultra-wideband (UWB) radar data with LIDAR data to enable safe navigation within vegetation. UWB radars typically operate at relatively low frequencies and are, therefore, able to penetrate vegetation. The proposed method augments LIDAR-based traversability maps with UWB radar data such that areas of obstacle-free foliage can be cleared. The resulting augmented traversability map captures the best properties of both sensors by exploiting the fine resolution of the LIDAR and the penetrability of the UWB radar.

Publication VI provides an improvement to Publication V by presenting an approach in which a machine learning is exploited to learn a sensor model for the UWB radar. The sensor model in Publication V was partly engineered manually and had to be tuned by the operator. Therefore, Publication VI proposes learning the UWB radar sensor model from experience, using a support vector machine (SVM) to significantly improve the classification accuracy.

Publication VII proposes a novel and efficient 3D representation for traversability analysis in outdoor environments that allows significantly lower map resolution compared to previous work. Furthermore, it proposes two new traversability classification methods based on this representation. These classification methods can classify sparsely vegetated areas as traversable without compromising accuracy on other terrain types. The proposed normal distributions transform traversability mapping (NDT-TM) representation exploits 3D LIDAR sensor data and extracts five different features for each map cell to perform the traversability classification: roughness, inclination, intensity mean, intensity variance, and permeability. Using these features, an SVM classifier is trained to discriminate between traversable and non-drivable areas of the NDT-TM maps.

1.4 The Author's Contributions

The scientific contributions of this thesis, ordered by the importance, can be summarized as follows:

1. Two innovative methods are proposed for augmenting LIDAR-based traversability maps with UWB radar data. The resulting augmented traversability maps enable safe navigation within densely vegetated environments, which has not been possible with current state-of-the-art methods (Publication V, Publication VI).

2. Efficient new representation (NDT-TM) is developed for large-scale 3D traversability mapping in unstructured environments allowing significantly lower map resolution than in previous work (Publication VII).

3. Two novel traversability classification methods are proposed based on the NDT-TM representation constructed from 3D LIDAR data. The proposed methods are able to classify sparsely vegetated areas as traversable, while still detecting partially visible objects, such as large rocks and tree stumps (Publication VII).

4. A novel human detection and tracking algorithm is developed that utilizes only radar data (Publication III).

5. The performance of the developed 2D LIDAR-based human detection method is analyzed and evaluated (Publication IV).

6. Software and hardware modules were developed for the control system and payload control of a generic off-road capable UGV that can operate with variable level of autonomy (Publication II).

7. A natural subsystem structure for UGV systems is proposed and analyzed (Publication II).

8. Different teleoperation delay sources are analyzed in a UGV application (Publication I).

1.5 Thesis Structure

The rest of this thesis is structured as follows. Chapter 2 gives an overview of the history of UGV systems and describes the state-of-the-art of UGV systems as well as events and trials that promote the development of such systems. Moreover, a natural subsystem structure for UGV systems is proposed and presented through a case study. Chapter 3 concentrates on the existing literature for human detection and traversability analysis methods. Since the literature of both these fields is vast, the survey's focus is on methods that are closely related to the novel methods this thesis proposes. Chapter 4 summarizes the main methods developed for human detection and traversability analysis in this thesis, whereas Chapter 5 presents the most important results from the experiments performed to validate these methods. Chapter 6 discusses the results and limitations of the proposed methods along with potential directions of future work. Chapter 7 concludes the thesis. The articles of this compilation thesis are attached after the Bibliography in the order listed in the List of Publications.

2. Unmanned Ground Vehicle Systems

This chapter presents a short history of unmanned ground vehicle systems (UGVs) and lists state-of-the-art UGV systems as well as events and trials that promote the development of such systems. Furthermore, it proposes a natural subsystem structure for UGV systems and presents this through a case study that includes a short analysis of different control modes for UGV systems.

2.1 Short History of UGVs

This section presents a short history of UGVs from the early days to the new millennium. The early experiments with radio-controlled vehicles are referred to, but this section's main emphasis is on the evolution of autonomous features on different UGV systems.

2.1.1 Early Days

The first driverless car was demonstrated already in 1925 when radio equipment firm Houdina Radio Control produced a radio-controlled vehicle that was driven through a traffic jam in New York City. The vehicle, known as American Wonder, was operated from a following car based on direct visual feedback (Time Magazine, 1925). Several other radio-controlled vehicles were presented in the following decades, including the Soviet TT-26 teletanks that were exploited in the Second World War (Czapla and Wrona, 2013). However, these radio-controlled vehicles do not fall under the UGV definition of this thesis, since they require direct visual contact between the controlled system and the operator.

The first ground vehicles that fit under our UGV definition were the Soviet lunar rovers Lunokhods that explored the moon in the early 1970s (Carrier, 1992). These rovers did not have any autonomous features but

were directly teleoperated by the operator based on transmitted camera images. In the early 1980s, the Navel Ocean Systems Center developed two teleoperated vehicles aimed for reconnaissance, surveillance, and target acquisition applications. The developed Ground Surveillance Robot and TeleOperated Dune Buggy were among the very first UGVs that were successfully teleoperated on the earth's surface. Both vehicles were driven with replicated control system based on stereo video feedback. (Gage, 1995)

2.1.2 Towards Full Autonomy

One of the earliest truly autonomous UGVs was the VaMoRs, a Mercedes van actuated for drive-by-wire capability and outfitted with a multiprocessor vision system. VaMoRs was developed at the Universität der Bundeswehr in Germany under the leadership of Ernts Dickmanns, a German pioneer of autonomous vehicles and computer vision. VaMoRs was able to drive at speeds up to $100\,km/h$ for more than $20\,km$ on an empty highway, based on computer vision, by 1987. (Dickmanns et al., 1990)

Meanwhile, a completely independent project with similar aims was carried out in the USA. It was initiated by the Defense Advanced Research Projects Agency (DARPA), an agency of the United States Department of Defense responsible for the development of emerging technologies. The huge Strategic Computing initiative, was designed to develop a new generation of machine intelligent technology. It contained one application area for Autonomous Land Vehicles (ALV) that focused on developing a broadly applicable autonomous navigation technology base. The developed eight-wheel vehicle, dubbed ALV, was able to safely steer along roads; avoided structured obstacles at low speeds by processing images from a rooftop closed-circuit camera. (Leighty, 1986)

Dickmanns' group demonstrated autonomous performance in normal highway traffic in 1994 with their new UGVs called VaMP and its twin VITA-II. These UGV's vision system recognized the road curvature, lane width, number of lanes, type of lane markings, vehicle pose relative to the lane and to the driveway, and the relative state of up to ten other vehicles. They successfully demonstrated autonomous lane changing, as well as free-lane driving and convoy driving at speeds up to $130\,km/h$ in normally dense, three-lane traffic. (Dickmanns, 1997)

The Robotics Institute (RI) at Carnegie Mellon University (CMU) built and studied computer-controlled vehicles for automated and assisted driv-

ing concurrently with the Dickmanns groups' work. The first autonomous vehicle they developed in 1986 was called Navlab (short for Navigation Laboratory) and looked like a standard commercial van from the outside with cameras and LIDAR mounted over the cab. The vehicle was equipped with hydraulic drive and electric steering that were computer controlled by electric and hydraulic servos. Moreover, the vehicle was equipped with three computers, an inertial measurement unit (IMU), a satellite positioning system, and gyrocompasses to enable autonomous navigation capability. There was room at the back for five researchers and observers, making Navlab a laboratory on wheels. (Thorpe et al., 1988)

Navlab had several different road following systems. The Autonomous Mail Vehicle system built a map of the traveled environment on the first run and reused that map later for positioning and road following when driving around the same area. The Generic Cross-Country Vehicle system utilized the vehicle sensors to build a 3D model of the surrounding environment in real-time and could plan and execute a local trajectory based on that model. The SCARF (Supervised classification Applied to Road Following) system tracked roads using adaptive color classification. The YARF (Yet Another Road Follower) system explicitly modeled as many aspects of road following as possible, for driving on structured roads (highways, freeways, rural roads, and suburban streets), which made the road following more robust (Amidi, 1990). The ALVINN (Autonomous Land Vehicle in a Neural Network) system was a road-following scheme based on a 3-layer back-propagation network that took input from the camera and LIDAR and produced the direction the vehicle should follow as an output. The network was trained using images, LIDAR data, and steering angles recorded while a human driver was driving the vehicle. (Pomerleau, 1989)

RI proceeded to build a series of 11 vehicles, Nablab 1 through Navlab 11. The applications included off-road scouting, automated highways, run-off-road collision prevention, and driver assistance for maneuvering in crowded city environments (Robotics Institute, 2012). Navlab 5 notably completed the No hands across America journey from Pittsburgh to San Diego in 1995 (over $4500\,km$) autonomously, which is considered one of the milestones of autonomous vehicles (Pomerleau and Jochem, 1996).

In the mean-time in Japan, Toyota developed a vision-based vehicle named the Automated Highway Vehicle System; it aimed at a possible solution to the issues caused by automobile traffic. The vehicle was able to

detect lane markings through a monochrome camera and keep the vehicle on the lane at speeds of $50\ km/h$. (Tsugawa, 1994)

An advanced perception and navigation system for UGVs operating in unstructured environments was developed around the same time in the PANORAMA project. The project was undertaken from 1989-1993 under the auspices of the European Community ESPRIT II program by an internationally distributed consortium comprising seven companies and seven research institutes from around the Europe. The main result of the large project was the modular perception and navigation system that achieved accurate navigation performance even when traveling long distances in difficult outdoor terrain. As a final demonstration, a full-scale rock-drilling machine performed an approximately one hour drilling mission (excluding drilling times) autonomously in an open quarry with significant elevation differences. (Halme and Koskinen, 1993)

2.1.3 New Millennium

During the decade on the 2000s, DARPA managed several programs and challenges that aimed to facilitate the development of UGV technology. DARPA launched Perception for Off-road Robotics program (PerceptOR) in 2001. PerceptOR sponsored three phases of development of autonomous outdoors mobility over four years. The core problem addressed in the program was the ability to drive long distances in challenging environments with minimal human intervention. CMU was again a major participant in the program, developing new approaches in planning, perception, localization, and control that were driven by the quest for reliable operation in challenging environments (Kelly et al., 2006). The typical performance by the end of the program in a challenging, unknown desert environment was an average speed of $66\ cm/s$, covering 90% of the distance in autonomous mode (Krotkov et al., 2007).

The PerceptOR program was followed by the Learning Applied to Ground Vehicles program (LAGR) that ran from 2004-2008. LAGR's goal was to accelerate the progress in autonomous, perception-based, off-road navigation in robotic UGVs. The main idea behind the program was to incorporate machine learning methods and to only use passive optical sensor systems to accomplish long-range scene analysis. Since the LAGR's goal was to create better navigation software rather than build custom hardware, DARPA commissioned a simple UGV known as the hHerminator, which was supplied to the participating teams. The

hHerminator is equipped with two stereo camera pairs for environment perception. Other on-board sensors include a Global Positioning System (GPS) receiver, an IMU, an infrared proximity sensor, and bumper-activated switches (Jackel et al., 2006). Eight teams were funded to develop software and, on approximately a monthly basis, the teams sent their software to DARPA, which conducted tests of all teams systems on a course of DARPA's choosing. The terrain typically varied from grass fields and trails through deciduous forest to desert scrub. Several impressive methods were developed during the program that focused on applying machine learning in off-road navigation of UGVs (Huang et al., 2009).

DARPA also sponsored a series of challenges for autonomous vehicles concurrent with the LAGR program. The DARPA Grand Challenge (DGC) competitions were held in 2004 and 2005 and the DARPA Urban Challenge (DUC) in 2007. The DGC's goal was to develop a mobile robot that can autonomously traverse an outdoor route of 140 miles consisting of dirt roads, trails, lakebeds, rocky terrain, and gullies. In the first DGC in 2004, 15 teams qualified for the main event, but no team could complete more than 7.9 miles of the course. The second DGC was held the following year, and 23 teams out of 195 applicants qualified for the final event. Remarkably, five vehicles successfully completed the course (Iagnemma and Buehler, 2006).

The five vehicles to complete the race were (from 1^{st} to 5^{th}) Stanley from the Stanford Racing Team (Thrun et al., 2006), Sandstrom and H1ghlander from the Red Team (Urmson et al., 2006), KAT-5 from Team Gray (Trepagnier et al., 2006), and TerraMax from Team TerraMax (Braid et al., 2006). Stanley took just under seven hours to complete the course, whereas the next three vehicles crossed the finish line 11, 20, and 36 minutes later, respectively. TerraMax completed the course in 12 hours and 51 minutes, which was over the time limit of 10 hours.

The DUC was held in a simulated, busy urban environment at the George Air Force Base in Victorville, California. The DUC's goal was to navigate through a mock city environment, executing simulated supply missions while merging into moving traffic, navigating traffic lights, negotiating busy intersections, and avoiding obstacles. There was a six hour time limit to complete the 60 mile course. Six teams out of 11 finalists completed the course, but only four of those were within the six hour time limit (Buehler et al., 2008).

The six vehicles to complete the race were (from 1^{st} to 6^{th}) Boss

from Tartan Racing (Urmson et al., 2008), Junior from Stanford Racing (Montemerlo et al., 2008), Odin from VictorTango (Bacha et al., 2008), Talos from MIT (Leonard et al., 2008), Little Ben from The Ben Franklin Racing Team (Bohren et al., 2008), and Skynet from Cornell (Miller et al., 2008). The winner, Boss, averaged approximately 14 miles per hour throughout the race and completed the race in 4 hours and 10 minutes, around 20 minutes before the second place Junior.

The success of the DGC and DUC accelerated the development of autonomous vehicles. One of the most notable achievements after the DUC was the VisLab Intercontinental Autonomous Challenge, the first intercontinental autonomous land journey conceived by VisLab (Artificial Vision and Intelligent Systems Laboratory, a spin-off company from the University of Parma) as an extreme test of autonomous vehicles. Four VisLab autonomous vehicles completed a trip of $13\,000$ kilometers from Parma, Italy, to Shanghai, China, in 2010, virtually without human intervention. All data were logged and used back in the laboratory to further improve the perception systems. (Bertozzi et al., 2013)

2.2 State-of-the-Art of UGV Systems

This section presents state-of-the-art UGV systems ranging from self-driving cars through industrial and off-road vehicles to legged robots. It also briefly mentions different events and challenges that promote the development of UGVs. UGV systems development is currently very rapid, and this section only gives an overview of some of the advanced UGV systems from around the world.

2.2.1 Self-Driving Cars

The achievements in DARPA's Grand and Urban challenges marked a significant milestone in robotics technology and escalated the development of autonomous self-driving cars. Shortly after the DARPA Urban Challenge (DUC), Sebastian Thrun — the team leader of the Stanford Racing team (winner of the DARPA Grand Challenge (DGC) 2005, runner-up in DUC) — joined Google to lead the Google self-driving car (SDC) project (Markoff, 2010). The Google SDC team is currently testing several SDCs on the streets of California, Texas, and Washington, and in February 2016, they reported that the fleet of SDCs has covered almost two and a half million

autonomous kilometers on public roads, latterly focusing mainly on city street driving (Google, 2016).

Baidu, the "Chinese Google", is also developing self-driving cars and has been testing their modified BMW 3-Series self-driving car on the streets of Beijing since December 2015. The company's deep learning laboratory has been working on this project since 2013 (Davies, 2015). Baidu recently received an Autonomous Vehicle Testing Permit from the California Department of Motor Vehicles, which allows them to also start testing their autonomous vehicles on California streets (Etherington, 2016).

Vislab had already presented their autonomous test vehicle BRAiVE (BRAin-drIVE) in 2008 that included 10 cameras and four LIDARs for perceiving the surrounding environment. VisLab performed large-scale experiments in downtown Parma in 2013, where BRAiVE successfully negotiated two-way narrow rural roads, traffic lights, pedestrian crossings, speed bumps, pedestrian areas, and tight roundabouts. VisLab engineers activated the vehicle in Parma University Campus and stopped it in the Piazza della Pilotta (downtown Parma). That was a 20-minute run in a real environment with real traffic at 11 am on a work day, and it required absolutely no human intervention (VisLab, 2013). VisLab unveiled their newest autonomous car, called DEEVA in 2014, which features over 20 cameras, 4 lasers, GPS receivers and an IMU. All sensors are fully integrated and enable the vehicle to cover a very detailed 360° view of the surroundings. (VisLab, 2014)

A test car from Uber's Advanced Technologies Center recently started driving around the streets of Pittsburgh collecting mapping data and testing its self-driving capabilities (Uber Newsroom, 2016). Uber and CMU established the Advanced Technologies Center in 2015 as a strategic partnership to focus on developing key, long-term technologies that advance Uber's mission of bringing safe, reliable transportation to everyone, everywhere (Spice et al., 2015). Furthermore, Uber's self-driving truck made its first delivery in October 2016, driving completely autonomously in highway traffic. The truck was retrofitted with a navigation system developed by San Francisco start-up Otto, which Uber bought in the summer of 2016. However, for the foreseeable future the driver remains an integral part of the system, since the navigation system only works in highway traffic (Davies, 2016).

nuTonomy launched the world's first public trial of a robo-taxi service in August 2016. The service is available for selected Singapore residents who can book a no-cost ride with the company's self-driving cars using a smartphone app. However, an engineer from nuTomony will ride in the vehicle to observe the system's performance and assume control if needed. nuTonomy will collect and evaluate data throughout the trial to refine the software in preparation for the launch of a widely-available robo-taxi service in Singapore in 2018. (nuTonomy, 2016)

One notable, government-driven effort to accelerate self-driving car technology is ongoing in Japan, where vehicles equipped with special surveying equipment started mapping the country's key expressways in September 2016. The plan is to utilize the generated high-definition 3D maps as part of a government campaign to have self-driving cars on the road before the 2020 summer Olympics, specifically to showcase Japan's advanced technology in front of world's media (Nikkei, 2016). Another reason to welcome self-driving cars in Japan its rapidly aging population. That is, self-driving cars are seen as a mean to diminish the car accidents caused by elderly and people suffering from dementia (Boyd, 2015).

All major car manufacturers have already developed autonomous features for their vehicles and have long-term plans to introduce fully autonomous vehicles. However, fully autonomous cars still have a legal battle to face. Currently, self-driving cars are only legal for road testing in a few states and cities worldwide. Therefore, in addition to the technical challenges still involved, the cars currently on the market only come with semi-autonomous features that assist the driver: for example, active blind spot assist, intelligent parking assist, adaptive cruise control, and active lane-keeping assist. Nonetheless, carmakers believe that fully autonomous cars could be ready for consumers within the next 5 to 10 years. Google believes that their autonomous vehicles will be available for consumers by 2020, and Elon Musk — the CEO of Tesla Motors — thinks that fully autonomous Teslas could be ready as soon as 2018. (Connor, 2015; McHugh, 2016)

Several technology companies provide subsystems today specifically developed for autonomous cars to further accelerate autonomous vehicle development. For example, NVIDIA provides powerful computing systems specifically designed for autonomous vehicles (NVIDIA, 2016), whereas Mobileye manufactures vision-based advanced driver-assistance systems (Mobileye, 2016). Nonetheless, in addition to the legal issues involved,

there are still some technical challenges to be solved before large-scale deployment of self-driving cars. For example, the difficult weather conditions caused several major problems for the competitors in Hyundai's competition for future automobile technology held in South Korea in 2014 (Ackerman, 2014).

2.2.2 UGVs in the Industry

UGVs with a high-level of autonomy are also extensively utilized at present in industry. Automatic Guided Vehicles (AGV) have been a common sight in factories for decades, and the mobile autonomous machinery has been moving out from factories to mones and harbors over the last decade, for example, where mobile machines with autonomous features have been incorporated into the daily operations. The first AGVs followed wires installed under factory floors, but modern AGV systems often navigate using beacon-based LIDAR navigation system (Martínez-Barberá and Herrero-Pérez, 2010). AGVs are widely used today in large-scale factories as a part of the manufacturing process.

Sandvik's AutoMine® is the world's first autonomous mining system, which today offers a wide range of different mining automation solutions, including loading, hauling, and surface drilling. All the automation solutions are fully scalable fleet automation systems in which one operator can manage several machines from the safety of a control room. The mining machines can navigating autonomously, localizing themselves by matching 2D LIDAR data against previously recorded data, but they are also teleoperable from the control room if needed. The autonomous machines need to be separated from people with a safety fence for safety reasons. Several AutoMine® systems are currently in use all over the world in dozens of mines. (Woof, 2005; Sandvik, 2016)

Harbor automation is currently increasing rapidly, and many operations, such as container transportation with straddle carriers, have already been automated in some container terminals. AutoStrad™ is a harbor automation system by Kalmar that was first taken into use in 2005 when Briabane's container terminal was automated. Since then the product family has diversified, and several other container terminals have been automated around the world. The navigation system of autonomous mobile harbor machines is based on high-end millimeter-wave radars and radar reflectors that are placed in known locations inside the harbor area. Radar sensors are exploited since they are practically immune to the dif-

ficult weather conditions often present at harbors. The automated harbor machines still need to be separated from people with a safety fence for the time being. (Kalmar Global, 2016)

Nonetheless, both autonomous mobile machinery in industry and self-driving cars have been developed to work only in structured environments. That is, self-driving cars are designed to operate on public roads and typically cannot negotiate off-road environments, whereas the unmanned vehicles in the industry are designed to work on very case-specific environments. For example, the harbor machines and mining machines are separated from people with a safety fence, since the reliability of human detection systems cannot yet ensure the safety of people at all times. Moreover, there are strong assumptions and requirements about the operating environment, such as the beacon network used by automated harbor machines. Autonomous navigation in an unknown off-road environment is one of the premier challenges in field robotics and requires more sophisticated navigation algorithms.

2.2.3 Off-Road Vehicles

Space robots are advanced UGVs specifically developed for unknown off-road conditions. For example, Mars rovers are very sophisticated pieces of technology that typically have a high level of autonomy. The latest Mars rover in operation is the Curiosity, which was developed by Jet Propulsion Laboratory (JPL) in cooperation with Boeing and Lockheed Martin. Curiosity already landed on Mars in 2012 and is still continuing its mission exploring previously unknown areas (NASA, 2016). However, the space robots are a very specific UGV subcategory and differ in many ways from UGVs operating on earth.

If we limit the UGV operating environment to earth, an Israeli border patrol robot, Guardium UGV by G-NIUS, is one of the most advanced off-road-capable autonomous UGVs available on the market. Guardium UGV is designed to patrol the Gaza border; the first batch of Guardiums were employed in 2008. The vehicle sensor suite includes a tactical positioning system, video and thermal cameras, and a sensitive microphone. Guardium can be directly teleoperated from the control station, and the vehicle can operate autonomously on- and off-road at speeds up to $80\ km/h$. (G-NIUS, 2016; Xin and Bin, 2013)

Agricultural robots are also among the most sophisticated UGVs currently operating in off-road environments. One of the first driverless

tractors was the APU-module developed from 1990-1995 by a Finnish company, Modulaire Oy. APU-module was able to autonomously navigate on a field using RTK-GPS and a digital guidance module (Nieminen and Sampo, 1993; Rintanen et al., 1996). Nowadays, several companies provide autonomous tractors, including Autonomous Tractor Corporation, whose AutoDrive promises highly precise, repeatable accuracy based on a laser-radio navigation system (Bedord, 2016). More experimental agricultural robots include the solar powered Ladybird and RIPPA robots, for example, developed at the Australian Centre for Field Robotics for optimizing crop yields. Both robots are equipped with an herbicide-spraying end effector that can deliver a controlled quantity of herbicide in exactly the correct position. The RIPPA drove autonomously up and down crop rows for over 21 hours in 2016 with an accuracy of $4\ cm$. (Bogue, 2016)

Several different UGVs have been developed for military and authoritative use over the last decade. However, most of these vehicles are either directly teleoperated or have a low-level of autonomy. For example, small, robotic building- and tunnel-searcher UGVs are extensively used by the U.S. military for short-range reconnaissance missions, but these UGVs are typically operated remotely by a soldier. (Pejic, 2016)

DARPA managed the UPI (UGCV PerceptOR Integration) program that developed a UGV in 2007 with one of today's most advanced off-road capabilities. UPI program built upon two previous DARPA programs — PerceptOR and the Unmanned Ground Combat Vehicle (UGCV) — and aimed to develop a highly mobile UGV capable of autonomously driving through deserts, mountains, forests, wetlands, and other challenging environments. (National Robotics Engineering Center, 2016)

The end result of the UGCV program was a UGV called Spinner, a highly durable, invertible, six-wheel-drive, hybrid-powered vehicle able to surmount challenging terrain obstacles. Furthermore, Spinner is easily teleoperated, tolerates occasional moderate crashes, and can recover quickly from such a crash (Bares et al., 2002; Bares and Stager, 2004). In the UPI program, the sophisticated software solutions developed in PerceptOR program were combined with the Spinner platform. The resulting two UGVs, called Crushers, combined the mobility and ruggedness of Spinner with advanced perception, autonomy, and learning techniques. The National Robotics Engineering Center (NREC), an operating unit within CMU's RI, led the development with several notable subcontractors (Carnegie Mellon Media Relations, 2006). However, the impressive

off-road capability of the Crushers was largely due to the advanced platform designed to surmount extremely challenging obstacles. That is, the Crushers did not need methods for evaluating obstacle-free vegetation, for example, since they could simply surmount all such obstacles.

A series of field experiments assessed the UPI program's mobility, autonomy, teleoperation, and mission capabilities in a variety of environments. The UPI program met or exceeded its ambitious performance milestones for speed and autonomous operation while remaining on schedule and within budget. The two Crusher vehicles logged more than a thousand kilometers across extreme terrain and averaged human intervention once every $20\,km$. The UPI program improved dramatically the speed, reliability, and autonomy of UGVs operating in extreme, off-road terrain. (Bagnell et al., 2010; National Robotics Engineering Center, 2016)

2.2.4 Events and Competitions for UGVs

In addition to DARPA's challenges, there have been several other competitions and events promoting the development of UGV technology over the past decade. Some of these competitions or events are arranged regularly and are a major driving force for UGV development. For example, RoboCup, a robotic competition concentrating on football playing robots, was founded in 1997 and has been held annually since then. Inspired by the Kobe earthquake in 2001, they incorporated a rescue robotics league to encourage UGV research in a socially significant, real-world domain. The challenges in RoboCup Rescue range from mechatronics for advanced locomotion over perception and planning up to providing full autonomy. (RoboCup, 2016; RoboCup Rescue, 2016)

The European Land Robot Trial (ELROB) is another annual event aimed at promoting the development of UGVs for task-oriented operation. ELROB is not an ordinary competition, as it allows the demonstration and comparison of UGVs in realistic scenarios and terrains. ELROB is designed to assess current technology to solve the problems at hand, using any appropriate strategy to achieve it; that is, direct teleoperation is permitted, but autonomous operation will be awarded in the scoring. The first ELROB was held in 2006 and has been held annually ever since. However, the event alternates between a military and a civilian focus each year. From 2013 onwards, the civilian event has been renewed and is called euRathlon. (ELROB, 2016)

euRathlon's vision is to provide real-world robotics challenges that will test the intelligence and autonomy of outdoor/off-road robots in demanding, mock disaster-response scenarios. The competition requires a team of land, underwater, and flying robots to work together to survey a scene, collect data, and identify critical hazards. The competition's focus in 2013 was on land-based vehicles, whereas in 2014 the competition addressed sea-based vehicles. The competition was held in 2015 as a joint land, sea, and air event for the first time. (Eurathlon, 2015)

The latest addition to the robotic events calendar is the RoboRace that will be held for the first time during 2016/2017 Formula E season. RoboRace is the first global, autonomous car racing championship in which completely autonomous electric cars capable of reaching top speeds of more than $300\,km/h$ compete in one-hour races designed to test artificial intelligence. All the teams will have the same car manufactured by a company called Kinetik, and they will compete using software rather than hardware. The races are planned to occur prior to each Formula E race on the same day using the same circuits. (Burgess, 2015, 2016)

2.2.5 Legged Robots

Despite some impressive achievements in autonomous off-road navigation, wheeled vehicles cannot negotiate some harsh environments; for example, mountainous forests are often inaccessible for wheeled vehicles. Plushtech Oy (today owned by John Deere) presented a prototype of a walking forest harvester in 1995 to address this issue. The development goal was to create a machine with the best possible working stability and minimum impact on the terrain. The six-legged machine adapts automatically to the forest floor and can move in any direction on the ground. A computer system controls all the walking motion, but an on-board operator controls both the direction of the movement and the boom operations. (Billingsley et al., 2008)

More recently, Boston Dynamics (acquired by Google in 2013) developed several legged robots that travel in outdoor terrain that is too steep, rutted, rocky, wet, muddy, and snowy for conventional ground vehicles. One of their first and, possibly the best known, robots is the Big Dog, a quadruped rough terrain robot that walks, runs, climbs and carries heavy loads. Big Dog's locomotion system includes joint position, joint force, ground contact, and ground load sensors, as well as a gyroscope, LIDAR, and stereo vision system. It can run around $6.5\,km/h$ and climb slopes up

to 35 degrees while carrying a $150\,kg$ load. (Raibert et al., 2008)

LS3 (Legged Squad Support Systems) is Big Dog's big brother designed for use by the U.S. Marine Corps. It can carry more load than Big Dog and can complete a 20-mile mission lasting 24 hours. LS3 incorporates an onboard vision system and GPS receiver that enable following a leader and autonomous navigation to designated locations. Cheetah is a tethered quadruped robot. the fastest legged robot in the world that can reach speeds over $45\,km/h$. The untethered version of Cheetah, called Wild Cat, currently can run around $26\,km/h$ (Boston Dynamics, 2013). The MIT researchers have also developed quadruped robots; their latest design, Cheetah 2, was successfully demonstrated recently as capable of jumping over obstacles over $45\,cm$ tall while maintaining a running speed of $8\,km/h$ (Chu, 2015; Park et al., 2015).

2.3 UGV System Structure

Developing algorithms for UGV systems requires a test bed capable of collecting data and validating the developed methods in a real environment. This section proposes a natural subsystem structure for UGV systems using the UGV demonstrator, an off-road capable UGV developed as a test bed for task-oriented operations, as an example.

All UGVs are complex systems comprising several subsystems. There are no standardized ways to define these subsystems, and different UGVs may differ significantly in the system structure. Most UGVs need similar functionalities, however, which induce the need for similar subsystems. Moreover, modularity must be applied whenever plausible to generate economically justified UGV systems (Ylönen, 2006). Publication II provides an overview of the development process of the UGV demonstrator, including an in-depth discussion of the vehicle's system structure. The article proposes a natural subsystem structure for UGV systems that include ten different subsystems. Figure 2.1 illustrates the UGV demonstrator subsystems and their interactions, while the following paragraphs explain the tasks and structure of different subsystems. Note, however, that the naming convention is not standard and subsystems with similar functionality might be named differently in the literature.

Locomotion system produces the motion of a UGV. Robotic applications use a wide range of different means to produce propulsion and motion. The UGV demonstrator was built on a commercial off-road vehi-

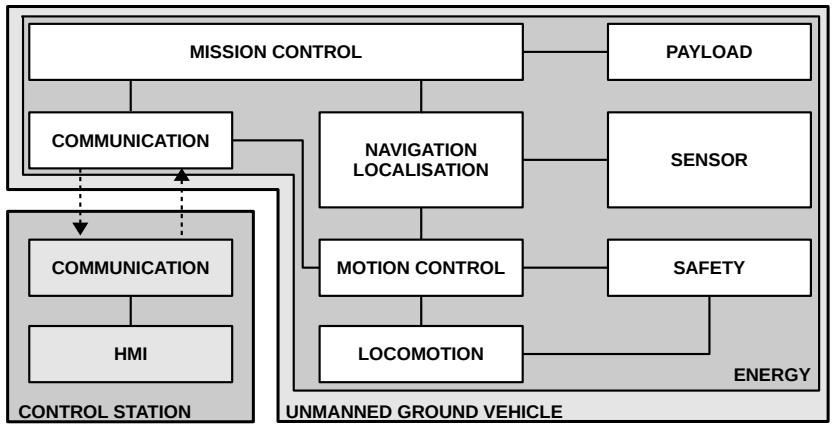

Figure 2.1. A block diagram illustrating the UGV demonstrator subsystems and their interactions.

cle; hence, the locomotion system consists of the vehicle platform together with the drive-by-wire instrumentation.

Energy system is responsible for providing power to all the other UGV subsystems. The main components of the UGV demonstrator energy system are two high-capacity electric batteries that are charged by a generator that is belt-driven by the vehicle engine.

Motion control system controls the UGV's movement by commanding the locomotion system according to higher level commands. In the UGV demonstrator, these commands may come from the operator in direct teleoperation mode or from the navigation system in autonomous operation mode. Furthermore, several semi-autonomous modes are available in which the navigation system assists the operator by taking over some part of the controls. The navigation system may be in charge of the velocity commands, for example, while the operator is responsible for the steering wheel control or vice versa.

Safety system is a critical part of any UGV and is responsible of stopping the vehicle in case of an unexpected event. If the vehicle computers are not working normally, for example, the vehicle should be stopped immediately. An emergency stop circuit (ESC) with no software in the loop was developed for the UGV demonstrator that overrides the motion control system when activated. The ESC monitors the state of the vehicle driving computer using an external watchdog circuit and activates if it observes abnormal behavior. Moreover, the ESC is activated if the system loses power, the connection to the remote control station is lost, or one of the emergency stop buttons mounted on the vehicle and the remote

control station is pressed. When the ESC is activated, the brake pedal is applied fully and the accelerator pedal is released.

Sensor system comprises all the sensors mounted on the UGV and provides the necessary data needed by the other subsystems. All UGVs need data from several sensors, regardless of the level of autonomy. The sensors on a UGV are proprioceptive (internal state) and exteroceptive (external state). Proprioceptive sensors measure values internally to the UGV, whereas exteroceptive sensors are used for the environmental observations. The typical sensor setup for UGVs with autonomous features includes at least the odometry sensors, an IMU, a global navigation satellite system (GNSS), vision sensor(s), and LIDAR(s). Many UGVs also incorporate other sensor modalities, for example, radar sensors. The UGV demonstrator sensor system incorporates two 2D LIDARs, two cameras, an IMU, odometry sensors, and a GPS receiver. Additionally, four low-quality cameras monitoring the vehicle's corners are available for the operator when in direct teleoperation mode. The LIDARs are mainly utilized in autonomous mode, whereas the cameras provide feedback for the operator in direct teleoperation mode.

Navigation system and **localisation system** are tightly coupled and form the heart of a UGV system. These systems are responsible for localizing the UGV and navigating to a desired target position. Many localization systems fuse data from the IMU, odometry sensors and GNSS receiver to form a pose estimation. However, depending on the quality of the available sensor data, this estimate may not be accurate enough; therefore, the localization system may need to resort to data matching techniques. The UGV demonstrator's localization system fuses data from a GPS-receiver, a high-end inertial positioning device, and the odometry sensors. The navigation system executes the path-following function to avoid obstacles based on the LIDAR data.

Mission control system is the high-level control system that provides instructions for the navigation system. Furthermore, it also provides instructions for the payload control system in case some payload is attached. The UGV demonstrator's mission control system receives the mission via a human-machine interface (HMI), divides the mission into smaller subtasks, relays the subtasks to appropriate subsystems, and monitors the subtask progress.

Payload control system is responsible for controlling any additional effectors that may be attached to a UGV. The payload can be anything

that enables the mission completion but is not needed by the other subsystems; for example, monitoring sensors, manipulators, and different tools (e.g., a grass cutter or a snowplough). The UGV demonstrator was developed for task-oriented operation and can perform various reconnaissance missions. The payload control system thus controls all the sensors related to these missions, that is, an NBC detector (Nuclear, Biological, and Chemical), a ground surveillance radar, and an observation camera.

Remote control station and **human-machine interface** are needed to communicate with a UGV. The remote control station can be as simple as a computer with a web connection and a simple browser-based user interface, in case of autonomous UGVs; however, in case the vehicle needs to be operated remotely, the remote control station needs to incorporate at least some control devices. The UGV demonstrator's control station consists of a laptop computer running the vehicle user interface, a steering wheel and pedals, and radio equipment. The HMI usability was tested in usability experiments; Publication II reports the results.

Communication system handles the communication between the UGV and the remote control station. Completely autonomous vehicles may not need to transfer any communication data, but a link to the vehicle is still a desirable option. The UGV demonstrator has two separate radio links: a short-range, high-bandwidth video-link for transmitting the video feed in direct teleoperation mode and a long-range, low-bandwidth radio used to transmit the command and control data. A long-range, high-bandwidth radio link would, ideally, handle all the data transfer; however, no feasible solutions were available at the time.

Direct teleoperation of a UGV requires relatively low communication delays, although the absolute requirements for the maximum delay depend on the task's nominal frequency (Suomela, 2004). Publication I analyzed the communication delay of the UGV demonstrator communication system in detail. Figure 2.2 summarizes the measured delays in direct teleoperation mode. It was noted that the delay in the system was still acceptable at lower speeds; however, the delay is a limiting factor for the vehicle top speed in direct teleoperation mode.

Nonetheless, the main part of the total delay is caused by the low-bandwidth radio link and could be decreased significantly by replacing the radio link with a modern high-bandwidth radio link. Moreover, introducing faster actuators would decrease the mechanical delay. The implementation of the UGV demonstrator was tried to keep it as light

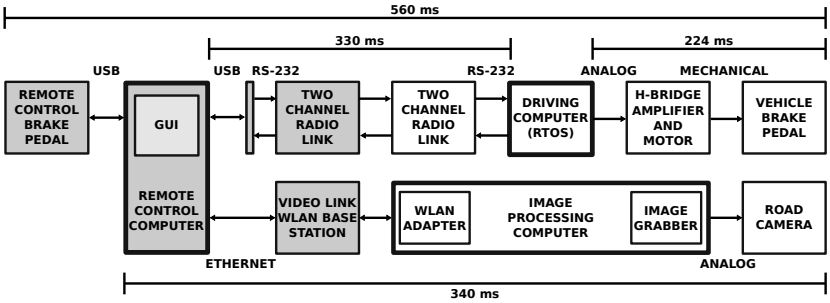

Figure 2.2. An illustration of the teleoperation delay sources analyzed in Publication I.

and cost-effective as possible, however, since the resources in the project were relatively limited and the project's primary interest was on tactical utilization scenarios of the UGV. Therefore, changing the hardware components was not an option, and other methods to tackle the delay are of interest.

Several different methods have been considered to overcome the problems associated with continuous closed-loop control over a time delay. The obvious option is to increase the level of autonomy; that is, instead of remaining within the continuous control loop, the operator can communicate only the goal and some instructions on getting there over the delayed communication channel. The operator still needs to continually monitor the performance and iteratively update or modify the task. The delay within the supervisory loop remains, but it is acceptable in most cases since there is no delay in the closed loop control and, thus, no instability. Another option is to use a predictor display, where the computer generates a visual indication of the motion and extrapolates it forward in time. This aids the operator by predicting what will happen, given the current state of the vehicle and the current control signal. (Sheridan, 1993)

A more recent idea to deal with teleoperation delay is virtual reality-aided teleoperation. Walter et al. (2004) proposed a virtual reality-based teleoperation system for UGVs that is designed to enhance operator's situational awareness. A large-scale, immersive virtual environment is used as the primary visual information source for the operator, which is augmented with sensor data from the vehicle. The system essentially deals with delay by enabling the operator to control a simulated vehicle in the future of the real vehicle. The trajectory of the simulated vehicle is provided as goal states for the real vehicle. The real vehicle reports sensor data back to the dynamics engine, which utilizes this information to predict the future position of the simulated vehicle. Walter et al. (2004)

reported promising preliminary results, in which delays up to ten seconds seemed to have no impact on task execution times when using the proposed virtual reality-based teleoperation system, while the task execution times for the direct, camera-based teleoperation system increased rapidly with only a modest increase in signal delay. The teleoperation delay should always be minimized from the usability perspective, however, despite the solid methods available for delay compensation. Nonetheless, if the price of hardware components that would reduce the delay is very high, applying delay compensation methods instead might be a viable option.

2.4 Modes of Control

The term teleoperation simply refers to the operation of a UGV system over a distance and, in a broad sense, all interaction with a UGV comes under this definition (Suomela, 2004). However, teleoperation in this thesis only refers to direct teleoperation when the operator is a constant part of a real-time control loop without a line of sight. Sheridan (1992) divided UGV control modes into manual control, supervisory control, and automatic control. That is, manual control is equivalent to the direct teleoperation definition of this thesis. According to Sheridan's definition, manual and supervisory control modes can be further divided, depending on the degree of computer control in the control loop.

The UGV demonstrator was designed to have several different modes of control; that is, there are intermediate supervisory control modes between direct teleoperation and fully autonomous mode in which the operator and the computer share the vehicle control. The transfer of control between a human operator and a computer, or the scalable level of autonomy, was one focus area in developing the UGV demonstrator. Scalable level of autonomy is used interchangeably in the literature with adjustable autonomy, as well as with sliding autonomy. It can be defined as the property of an autonomous system to change its level of autonomy to one of many levels while the system operates (Dorains et al., 1998).

The UGV demonstrator has four different control: direct teleoperation, cruise control, waypoint following, and fully autonomous. The vehicle control system is controlled directly from the remote control station in direct teleoperation, whereas the vehicle speed is automatically maintained by the driving computer in cruise control mode. Velocity control is left for

the operator in the waypoint following mode, but the vehicle automatically follows a predefined route. The vehicle follows waypoints in the fully autonomous mode, adjusting also the vehicle velocity automatically, leaving only the vehicle's supervision to the operator.

However, based on the usability experiments performed with the UGV demonstrator (reported in Publication II), it was evident that the human-machine interaction could be further improved to enable more flexible mission completion. On the one hand, it was noted that the modes of control should be kept low to keep the interface simple; on the other hand, the test subjects identified the need for additional modes. One key observation was that the information transmitted to the remote control station was insufficient for reliable obstacle detection or identifying traversable areas. One improvement idea was to add a control mode in which the computer would automatically assist the operator by detecting obstacles (particularly humans) and traversable areas and augmenting the camera images transmitted to the remote control station by highlighting these detections. The rest of this thesis discusses developing algorithms for automatically detecting both obstacles (including human detection) and traversable areas from sensor data.

3. Human Detection and Terrain Traversability Analysis Methods in Robotic Applications

This chapter gives a brief review of the relevant literature related to human detection and terrain traversability analysis methods in the context of unmanned ground vehicles (UGVs). Special attention is given to the areas related to the publications of this thesis, that is, human detection without vision-based sensors and traversability analysis in vegetated environments.

3.1 Human Detection Methods

The detection of humans or pedestrians has been studied extensively in the robotic community since, it is considered one of the fundamental problems in robotics. The ability to accurately detect and track humans still presents a major barrier to the large-scale deployment of UGVs in populated environments. The main challenge in human detection originates from the wide variety of positions and appearances that people can assume. A moving sensor system and stationary people further complicate the task. People trackers are often incorporated into the human detection systems, since tracking enables acceptable performance in the presence of occlusions and of occasionally missed people. Nonetheless, also people tracking is challenging, because human behavior can be completely unpredictable. The following subsection presents state-of-the-art methods in human detection by providing a brief overview of vision-based human detection methods and focusing more thoroughly on methods that exploit other sensor modalities.

3.1.1 Human Detection Incorporating Vision Sensor

Most human detection systems incorporate vision-based solutions due to the high information content of image data. Several different approaches

exist for visual human detection but, broadly speaking, they can be divided into two categories: human detection methods that try to detect the whole human body and methods that aggregate evidence from separate body-part detectors. The majority of the methods from both categories exploit traditional machine learning approaches and follow three main steps. First, a feature extractor is designed that converts the raw data into suitable, informative feature vectors. Second, a classifier is trained based on the features extracted from labeled training data, utilizing a suitable machine learning method. Third, the performance of the classifier is validated using labeled validation data. The classifier is ready for use when the validation data results are satisfactory. (Gerónimo and López, 2014)

However, deep networks (typically convolutional neural networks (CNN)) have recently gained more popularity in human detection applications. The main benefit of deep learning methods is that they obviate feature engineering; that is, deep learning algorithms learn informative features from the data and do not need hand-crafted feature representation. Convolutional layers in CNN are exceptionally good at finding good features in images to the next layer to form a hierarchy of nonlinear features that grow in complexity (e.g., edges, blobs –> noses, eyes –> faces). The performance of deep learning systems seem to be bound only by the amount and quality of training data, whereas traditional machine learning methods cannot improve after a certain amount of data (LeCun et al., 2015). Nonetheless, the current state-of-the-art results of different vision-based human detection methods are still relatively close, and no method is clearly superior to others. Furthermore, despite the absence of feature engineering, designing and training deep networks still requires deep domain expertise, a lot of data, and plenty of computational resources. Comprehensive reviews of different vision-based human detection solutions can be found in Schiele et al. (2009) and Benenson et al. (2014).

Another common approach for detecting and tracking people is to use a range sensor, such as radar or LIDAR, as a primary object detection module to limit the search space, and a camera for the classification. Good examples of such systems can be found in Milch and Behrens (2001), Kobilarov et al. (2006), and Premebida et al. (2014) where a vision sensor was fused together with a radar, 2D LIDAR, and 3D LIDAR, respectively. Another option is to utilize an RGB-D sensor (i.e., range camera; red, green, blue - depth), which eliminates the need to calibrate and synchro-

nize two separate sensors. For example, after the introduction of Kinect, a relatively economical RGB-D sensor developed for Xbox by Microsoft, it has also been widely utilized in robotics (Han et al., 2013). For example, Xia et al. (2011) exploited the Kinect depth information to detect humans, whereas Spinello and Arras (2011) proposed a method that relies on both the depth and the RGB data as sensory cues. Unfortunately, Kinect does not work in direct sun light, and the maximum detection range is only a few meters. Some other types of depth cameras remain operational in direct sunlight, but typically the range is still a limiting factor.

However, systems that rely on vision sensors have a major drawback: they do not work in the dark (without active lighting), and their performance is significantly affected by the changes in illumination. Adverse weather conditions also deteriorate their performance; moreover, camera-based human detection requires a lot of processing power, which might be a limiting factor in some applications. Therefore, a clear need exists for human detection methods utilizing other sensor modalities besides cameras.

3.1.2 LIDAR-Based Human Detection

Most UGVs are equipped with LIDARs, which makes them appealing sensors for human detection. Moreover, LIDARs provide accurate measurements, typically have a long detection range and wide field-of-view (FOV), and are immune to the changes in the illumination.

Affordable 2D LIDARs typically provide sufficient information for human detection when a UGV is operating on a relatively smooth structured area. The human detection method depends significantly on the mounting height of the LIDAR. The sensors are mounted at the height of the human torso in many 2D LIDAR-based human detection approaches, such that the LIDAR is looking over most of the common objects and obstacles in a typical indoor environment. These approaches extract people from sensor data as single clusters, which are then tracked with a filter (Kluge et al., 2001; Topp and Christensen, 2005). Similarly, Mucientes and Burgard (2006) extracted single clusters, but they also tracked the moving clusters whenever they were in close proximity to each other, based on the assumption that people tend to move around in groups.

However, a 2D LIDAR system is typically mounted at lower level for navigation and obstacle detection purposes. The human detection method in these cases must concentrate on finding leg hypotheses as

in Kleinehagenbrock et al. (2002); Schulz et al. (2003); Scheutz et al. (2004); Lee et al. (2006); Chung et al. (2012). Distinctive features need to be extracted from the LIDAR data to distinguish humans from other objects; both geometric and motion features are usually exploited. The downside with the motion features is that they can only detect moving people. Overall, selecting suitable features and tuning the algorithm is challenging; thus, machine learning approaches have been utilized to learn the classification model from the data.

Luber et al. (2009) described an exemplar-based model of dynamic objects, such as humans, and employed an unsupervised learning approach for the model-building problem. However, this method is not able to classify humans from other dynamic objects. Arras et al. (2007) defined a list of 14 geometrical and statistical features and used supervised learning to create a classifier for detecting people. Arras et al. (2008) subsequently applied multi-hypothesis tracking (MHT) algorithm for data association and tracked the detected legs separately. A person track was created if two tracks were sufficiently close to each other and moved in the same direction for a certain period of time. Arras et al. (2012) recently proposed a method for learning a strong classifier by combining a set of weak classifiers based on the geometrical and statistical features. Moreover, they further extended their MHT algorithm for tracking groups of people as well as incorporating adaptive occlusion properties.

Publication IV proposed a leg tracker-based human detector that exploits similar principles as in Arras et al. (2008); however, that method is computationally significantly lighter, which makes it well suited for applications with limited computation resources. Leigh et al. (2015) proposed a novel method for person tracking and following that exploits similar features. They reported improved accuracy and a reduced number of errors compared to previous work. The computational complexity of their approach is lower than in Arras et al. (2012), but remains significantly higher than with the method Publication IV proposed.

Information from a 2D LIDAR is not always sufficient, especially for mobile platforms operating on uneven terrains. For example, Navarro-Serment et al. (2010) exploited the geometric and motion features from a 3D LIDAR data to recognize human signatures in complex environments. Spinello et al. (2010) used a supervised learning approach to create a bank of classifiers for different height levels of human body based on 3D LIDAR data, whereas Bohlmann et al. (2013) utilized a 3D LIDAR

for robust autonomous person following outdoors. Prokhorov (2009) used Recursive Neural Network (RNN) to detect objects, such as humans, from 3D LIDAR data; however, the main contribution of Prokhorov (2009) was how to handle the rotation invariance. On the downside, 3D LIDARs are expensive sensors, which limits their deployment in consumer robotics.

3.1.3 Radar-Based Human Detection

Radars typically provide reliable measurements regardless of the weather conditions, which make them also a desirable sensor option for human detection system; however, classifying targets as humans using only radar data is a challenging task. Nonetheless, there are at least three different kinds of techniques applied to this problem. Yarovoy et al. (2008) measured the reflectivity of a human in laboratory conditions with ultra-wideband (UWB) radar; by analyzing the polarization of the reflected signal, they discovered that there are some frequencies where one polarization has a maximum reflectivity, while the other has a minimum reflectivity. However, the polarized signal depends strongly on the shape, posture, and position of the person, which makes it very unreliable method for human classification.

Nakane and Soshi (1998, 2000) used a dual band frequency modulated continuous wave (FMCW) radar to discriminate whether or not detected objects are animals, including humans. They compared the difference in the power of the signal reflected from an object at different frequencies ($10\,GHz$ and $60\,GHz$) and were able to establish a threshold for the ratio of received intensity between two frequencies, above which the detected objects can be identified as animals.

Otero (2000) analyzed the Doppler spectrum of FMCW radar to obtain a Doppler signature for a walking human. The movement of a walking human's legs, arms and torso cause different components to the Doppler frequency. The motion of the torso produce a steady Doppler shifted signal, which is modulated by the motion of swinging arms and legs that results in a Doppler signature that is very characteristic of humans. Otero (2000) proposed a simple, binary classifier that classifies detection as either a person present or not present.

Gürbüz et al. (2007) evaluated different methods used to detect walking humans from the Doppler data with the conclusion that spectrogram based methods are problematic if one needs to distinguish human from other periodically moving targets due to their high signal-to-noise ratio.

Distinguishing the targets based on the Doppler signature is problematic in the case of multiple targets in the radar FOV, since the spectral signatures are superimposed together. However, the Doppler spectrum still offers important evidence. Publication III presented a human detection and tracking system in which FMCW radar was utilized to detect and track objects within the FOV; both the Doppler signature and the target speed were analyzed to provide evidence of whether or not the target is a human.

3.2 Terrain Traversability Analysis

Terrain traversability analysis is used as a means to generate traversability maps of the environment that quantify the difficulty a UGV would encounter in passing through a particular region. Traversability maps are typically platform dependent, since the locomotion capabilities of different-sized platforms may differ significantly (Molino et al., 2007). The essence of traversability analysis is deducing whether an area is traversable or not, given the platform constraints and sensor data. This is an easy task in simple structured environment; however, estimating terrain traversability in natural off-road environments is extremely challenging due to the terrain's highly variable appearance and geometric properties. For example, vegetation is often interpreted as obstacles by the state-of-the-art methods, even though in practice it is often possible to drive through sparse vegetation. Conversely, this is also a challenging task for human drivers, since we cannot always see obstacles behind vegetation. Human drivers typically tend to adjust their speed in situations with limited visibility of the area ahead so they can to stop if they detect an obstacle (Schreuder, 1991). This could, however, could lead to avoiding even traversable vegetated areas altogether.

Nonetheless, a representative spatial model of the surrounding environment is needed to generate traversability maps; therefore, this section reviews the relevant contributions in the area of spatial modeling, as well as in terrain traversability analysis. Vegetation classification and traversability analysis within vegetated areas receive special attention, since traversing in vegetated environments is particularly challenging for UGVs.

3.2.1 Spatial Modeling

Occupancy grid mapping, originally introduced by Moravec and Elfes (1985), is one of the most predominant spatial modeling techniques in robotics applications. Occupancy grid maps represent the environment as a regular grid, in which each grid cell models its probability of being occupied. Occupancy grids were originally used as a 2D modeling tool, but they are easily scalable to three dimensions. However, 3D occupancy grids require a lot of memory, thus rendering them infeasible for large-scale mapping applications. Octomap (Hornung et al., 2013), a popular implementation of 3D occupancy maps, is based on an octree grid structure. Octrees have natural multi-resolution support, which provides an efficient way to maintain unobserved portions of the map, thus reducing the memory requirements.

The elevation map is a grid-based, 2.5D spatial representation, in which each cell in the 2D grid stores the height of the surface in the corresponding area (Siciliano and Khatib, 2008). Elevation maps have been popular mapping tools for outdoor applications since the early years of robotics. Bares et al. (1989), for example, used an elevation map for footstep placement selection of a legged planetary rover. However, the elevation map representation reduces the dimensionality from 3D to 2.5D. That is, it can only model a single surface per cell. Therefore, elevation maps cannot correctly model overhanging structures (e.g., bridges, tunnels, tree branches). Another drawback of elevation mapping is that it cannot reliably express the height of areas with little or no data.

Lang et al. (2007) proposed using adaptive non-stationary kernel regression in Gaussian Processes (GPs) to take the missing data problem into consideration and to deal with varying data densities in terrain models. The central idea of GP terrain modeling is to represent the height value of each point as a function of its 2D space coordinates and to subsequently approximate the value using a set of Gaussian distributions in function space. The available sensor data are used to learn the hyperparameters of a GP, which can then be used to perform regression for any point in 2D space and obtain an interpolated height value, resulting in a continuous spatial model. For example, Vasudevan et al. (2009) proposed an approach for modeling large-scale and complex terrain using a single neural network-based GP, which they demonstrate to preserve many

of the spatial features in the terrain. Hadsell et al. (2010) extended the traditional kernel-based learning approaches to estimate continuous surfaces by providing upper and lower bounds on the surface. This was done by exploiting the sensor's visibility constraints with respect to the terrain surface and, subsequently, applying kernel-based regression techniques to improve the precision of the terrain geometry estimate.

Triebel et al. (2006) proposed multi-level surface (MLS) maps to relax the functional constraint of a single height value per location of GPs and elevation mapping; this was and extension of elevation mapping, wherein each cell can store multiple height values. The proposed model was used to perform localization and navigation in an outdoor environment with several overhanging obstacles, where the robot successfully traversed across and under a bridge at the site.

Polygonal meshes are another spatial representation method that is particularly popular within the computer graphics community. A polygonal mesh is a graph of interconnected vertices in which each polygon represents a facet in the mesh. Special care must be taken in data filtering and handling of mesh uncertainty to generate the best reconstruction result from noisy point cloud data. For example, Wiemann et al. (2010) presented a method to automatically generate triangle meshes from noisy registered point cloud data. However, the resulting triangle mesh was generated as a post-processing step and was not maintained online. Rusu et al. (2009) proposed a complete pipeline from sensor data to localization, mapping, and path planning, in which the maintained map is a polygonal mesh generated from point cloud data. Similarly, Garrido et al. (2013) exploited triangle meshes representing 3D surfaces to perform path planning for robots operating outdoors.

The Normal Distributions Transform (NDT) is a compact spatial representation originally introduced by Biber and Strasser (2003) in the context of 2D scan matching. NDT is a grid-based representation, much like occupancy grid maps but capable of obtaining similar accuracy while using much larger cell size (Stoyanov et al., 2013). The NDT's key idea is that the observed range points are represented as a set of Gaussian probability distributions computed for each cell; that is, each distribution describes the probability of a point being measured at a particular physical location. NDT Occupancy Map (NDT-OM) is an extended NDT map that enables recursive updates of sequential measurements; it also models the cell's occupancy probability (Saarinen et al., 2013). As a result, NDT-OM

is an efficient representation for long-term large-scale mapping, which maintains its consistency even in dynamic environments. Additionally, Stoyanov et al. (2013) demonstrated that NDT spatial models allow significantly lower resolution to be used compared to other state-of-the-art 3D spatial modeling techniques without compromising the model's accuracy.

3.2.2 Traversability Analysis

Different traversability analysis methods were classified in a recent survey by Papadakis (2013) into three major constituents, namely, proprioceptive, appearance-based, and geometry-based approaches, with the latter two comprising the domain of exteroceptive approaches. Furthermore, Papadakis (2013) noted that hybrid approaches do exist that may further imply the use of additional sensor modalities other than LIDARs, cameras, or proprioceptive sensors. Traversability analysis methods typically exploit only data from onboard sensors, but attempts have also been made to link a priori information, for example, from satellite images with local classification to improve long distance traversability estimates (Bagnell et al., 2010).

Proprioceptive Approaches

Traversability analysis methods based on proprioceptive sensing are useful in learning models that capture the difficulty encountered while a vehicle is traversing a given terrain. For example, Martin et al. (2013) constructed large-scale traversability maps for vehicles performing repeated activity in a bounded environment; these maps are based on the vehicle power consumption, longitudinal slip, lateral slip, and vehicle orientation. Leppänen (2007) in contrast, exploited proprioceptive sensors to measure the interaction between the terrain and a wheel-legged robot to change the mode of locomotion between driving, walking, and rolking (rolling-walking), depending on the roughness of the terrain ahead.

However, proprioceptive sensors have a very limited capability to predict the terrain traversability that is about to be visited. That is, if the sensors indicate that the ground underneath turns softer, it might signify that the terrain ahead is even softer and might not be easily traversable for the robot. Nonetheless, such predictions come with high uncertainty, and the predictions are applicable only for very short ranges. Thus, proprioceptive sensors generally cannot be used to assess the

drivability of the robot surroundings; therefore, proprioceptive sensing should be further combined with long-range sensing modalities to avoid possible collisions with obstacles. Howard et al. (2006), for example, proposed a learning method that associates proprioceptive sensor data underfoot with previously acquired visual information of the same terrain to train a model for predicting terrain properties from visual appearance only. Similar approaches were also presented by Kim et al. (2006) and Bajracharya et al. (2009).

Appearance-Based Approaches

Appearance-based approaches to traversability analysis reformulate the problem as an image-processing and classification task; thus, they usually choose between a discrete set of terrain classes, rather than regressing on traversability. For example, Angelova et al. (2007) proposed a method for learning a hierarchical classifier for color images to differentiate between sand, soil, asphalt, grass, woodchip, and gravel. Kim et al. (2007) performed natural terrain classification between traversable and non-traversable regions by using super-pixels extracted from an over-segmentation of an image. This showed that these regions of homogeneous visual content are superior to rectangular image patches that are typically sensitive to the tessellation resolution and occlusions.

However, an evident complementarity exists between range sensors and image sensors, which several works have exploited to increase the overall robustness or extend the range of operations. For example, Happold et al. (2006), Shneier et al. (2008), and Zhou et al. (2012) all proposed methods based on the assumption that similar looking regions have similar traversability. They trained image-based traversability classifiers using range data only in the training phase. Happold et al. (2006) combined unsupervised learning of color models that predict scene geometry with supervised learning of the relationship between geometric features and traversability. They trained a neural network offline on hand-labeled geometric features extracted from range data and applied an online process for learning the association between color and geometry, which enabled the robot to estimate terrain traversability based only on the color data. Shneier et al. (2008) proposed a method for learning a classifier for color images that predicts the traversability of regions using only the image data. The range sensor data were used in the training phase to locate regions corresponding to ground

and obstacles that were used, along with the color and range data, to construct models of the regions' appearance. Zhou et al. (2012) introduced a self-supervised sensing approach employing both LIDAR and vision sensors that attempts to robustly identify a drivable terrain surface for UGVs operating in forested terrain. The LIDAR data were exploited to train a visual classifier to discriminate between the ground and non-ground regions in the image, but the final terrain class prediction was performed solely from visual data. Recently, Cunningham et al. (2015) proposed an interesting method for detecting the difference between traversable, compact soil and loose, hazardous soil by remotely estimating terrain diffusivity. They analyzed the thermal transient introduced by a continuous-wave laser and measured by a thermal camera.

Geometry-Based Approaches

The majority of terrain traversability analysis methodologies are based on geometric processing, although the geometric information is often fused with other sensor modalities to improve the classification robustness. A terrain model is typically built from 3D data and used to extract a set of features. More complex and higher level processing could be pursued on top of such a model by further taking into account a robot model, as well as stability and kinematic constraints.

One of the early approaches for geometric traversability analysis is to compute gradients for each cell in an elevation map, which are then compared against platform-specific thresholds (Chang et al., 1999). Another similar approach is to compute a traversability index for each cell in an elevation map using the terrain's slope and roughness (Ye and Borenstein, 2004). Thrun et al. (2006) proposed a more probabilistic grid-based approach that formed the base for the terrain analysis module of the vehicle Stanley that won the DARPA Grand Challenge. This approach labels the cells as free, occupied, or unknown, based on the vertical distance between nearby 3D LIDAR points. A probabilistic model was developed to take the errors in the robot's pose estimation into account.

Vandapel et al. (2004) presented a method that uses local 3D point statistics to segment LIDAR data into three classes: clutter to capture grass and tree canopy, linear to capture thin objects like wires or tree branches, and surface to capture solid objects like ground terrain surface, rocks or tree trunks. Lalonde et al. (2006) similarly classified 3D LIDAR data online, based on their salient features (i.e., scatterness, sur-

faceness, and linearness). These features were computed using principal component analysis (PCA) of the neighboring 3D points. Gaussian Mixture Models (GMMs) for these classes were learned by employing expectation maximization on these features. The classification results were filtered to account for outliers in the results, after which the ground was discriminated from other surfaces.

Santamaria-Navarro et al. (2015) presented a high-level, offline classification mechanism that learns traversable regions from large 3D point clouds gathered with a 3D LIDAR. The traversability is modeled as a GP and trained with an automatically labeled data set. The classification step exploits slope and roughness values that are computed for all the points using PCA. Two different classification approaches were proposed. The first employs GP regression and relies only on positive teaching samples collected from the robot footprints. The second approach performs GP classification that requires teaching samples from both classes. The remaining unlabeled points are randomly sampled, therefore, to acquire the negative teaching examples. It was shown that the GP classification, although computationally more expensive, increases the classification accuracy.

Terrain traversability analysis within the NDT framework was first addressed by Magnusson (2009) and Stoyanov et al. (2010), whereby a proposed constant threshold classifier (CTC) algorithm compares the roughness and inclination calculated from each cell distribution against predefined thresholds to generate a traversability map for path planning purposes. These features are determined based on the eigenvectors and eigenvalues of the covariance matrices associated with each cell. Publication VII proposed a Normal Distributions Transform Traversability Mapping (NDT-TM) representation for 3D traversability mapping in unstructured natural environments that extends the previous representations by adding intensity distribution and expected permeability as features. It furthermore proposed two classification methods exploiting this representation. The CTC algorithm has been shown to perform well in a structured environment, but it underperforms in unstructured environments. The classification methods proposed in Publication VII improve the classification accuracy significantly in complex environments. Figure 3.1 shows an example of an NDT-TM with an aerial photograph of the test environment and an NDT-OM color coded by height. The aerial photograph was taken about a month before the experiments and, there-

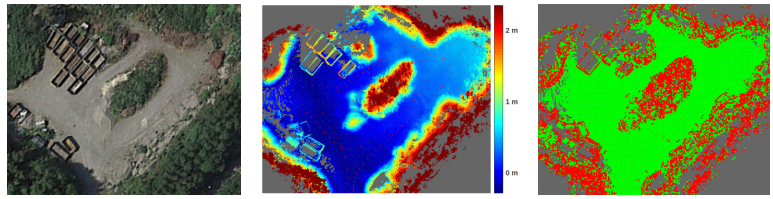

(a) (b) (c)

Figure 3.1. An example of NDT maps. (a) An aerial photograph (© Google) of a test environment. (b) A top-down view of an NDT-OM generated from 3D LIDAR data from the test environment color coded by height. The red dots illustrate the UGV trajectory during the experiment. (c) A top-down view of an NDT-TM from the environment colored by traversability (green means traversable, red means non-traversable).

fore, the environment depicted in the photograph differs slightly from the mapped environment.

3.2.3 Vegetation Detection

Most of the current traversability analysis methods consider obstacles as rigid and static; these fail to deal with vegetation-like obstacles. This problem has been approached by classifying vegetation to distinguish it from other types of obstacles. One often exploited property of vegetation is the reflectance of chlorophyll, which is found in living plants, that strongly reflects near-infrared (NIR) light but absorbs blue and red visible light (Myneni and Hall, 1995). For example, Bradley et al. (2004) presented a multi-spectral, camera-based solution for detecting chlorophyll-rich vegetation based on NIR light reflectance properties. Vegetation was detected by subtracting each pixel in the red channel of the visible-light image from the corresponding pixel in the near-infrared image and thresholding the result. Wurm et al. (2014) also exploited chlorophyll's reflectivity, whereby a support vector machine-based classifier was trained to classify grass in semi-structured environments, such as parks. The classifier was trained in a self-supervised way by employing a vibration-based classifier to detect the surface type currently traversed by the robot.

Nguyen et al. (2012a) proposed to detect vegetation in unstructured environments using a spreading algorithm to identify color and texture dissimilarities between the neighboring pixels in multispectral images. The seed pixels from which the spreading search is started, are selected by thresholding chlorophyll-rich vegetation pixels. Another spreading algorithm is carried out in parallel based on spectral reflectance. The

results from the parallel spreading searches are combined to form the final classification. The approach is reported to result in vegetation detection robust to illumination effects. In previous work the authors presented a method to double check the passable vegetation by mounting an air compressor device in front of the vehicle and utilizing motion detection techniques to confirm the vegetation classification (Nguyen et al., 2012b).

Another property of vegetation is that, unlike solid obstacles, range measurements often penetrate sparse vegetation. Lacaze et al. (2002) first exploited this property by counting the hits and misses of laser beams in cells in a voxel grid, then using the obtained density value to classify solid obstacles. Macedo et al. (2000) presented a statistical analysis of the range data produced by 2D LIDAR, with the goal of determining whether an obstacle is a rock (non-traversable) or a patch of grass (traversable). The proposed classifier compares local estimates of the variance and the skewness of the range distribution to predefined thresholds, resulting in robust classification even if the obstacles are partially occluded by vegetation. Castano and Matthies (2003) proposed a related approach, applied to real-time foliage detection from 2D LIDAR measurements. They used the expected localities and continuities of an obstacle, both in space and time, in contrast to the work of Macedo et al. (2000). The method first identifies those returns likely to be obstacles and then prunes them to eliminate false positives. The ability of LIDAR rays to penetrate foliage has also been extensively exploited in remote sensing where airborne LIDARs are utilized to create digital elevation models (DEM). Unlike photogrammetry, airborne LIDARs can be used to create DEMs even in forested areas due to LIDAR's ability to penetrate canopy (Liu, 2008).

Bajracharya et al. (2013) proposed a stereo vision-based terrain mapping system used by a legged vehicle able to detect sparse structures, such as vegetation, that do not present a hazard to the robot. The key insight is that such structures tend be thin; that is, these objects have a large number of depth discontinuities in the stereo coverage. Furthermore, they typically have high texture, implying that they should have dense stereo coverage. The presented method exploits these phenomena by processing the disparity and rectified image directly and then projecting occurrences into the map to accumulate their statistics. The system can operate during night time using NIR illuminators.

Wellington and Stentz (2004) proposed a method for predicting the load-bearing surface within vegetation. They apply an online adaptive method to learn from experience the mapping between the real ground height and the LIDAR measurements. The environment is modeled as a set of voxels, and the number of LIDAR pass-throughs (number of LIDAR rays passing through the voxel) is recorded, along with the LIDAR rays that hit the voxel. Voxels that contain a mixture of hits and misses are then assumed to contain vegetation. The proposed approach also exploits the maximum laser remission values, simple statistics on height, and the salient features, as in Lalonde et al. (2006), using a similar resolution.

Wellington (2005) and Wellington et al. (2006) proposed a terrain model in subsequent work that includes spatial constraints. The work introduced Markov Random Field (MRF) models and Hidden Semi-Markov Model (HSMM) to the terrain's 3D structure. The Markov random fields encode the assumptions that ground heights vary smoothly and terrain classes tend to cluster. They also incorporated infrared temperature and color information as additional features in this work.

Unfortunately, it is not always enough for safe navigation to be able to distinguish vegetation from other obstacles, since there might be an obstacle hidden behind the vegetation. Publication V and Publication VI addressed this problem, whereby UWB radar was utilized in parallel with LIDAR to augment traversability maps in vegetated environments. It was shown that since the utilized UWB radars can penetrate around $40\ cm$ of vegetation, it is possible to generate accurate traversability maps of densely vegetated environments such that solid obstacles hidden behind dense vegetation can still be detected.

3.3 Open Research Questions

Human detection has come a long way in recent years, and impressive results have been achieved with state-of-the-art methods. However, the majority of human detection methods still rely mostly on vision-based detection methods that have major drawbacks. That is, illumination changes and adverse weather conditions significantly affect their performance. Moreover, vision-based solutions are typically computationally expensive and, therefore, cannot be applied in systems with limited computational resources. Thus, utilizing other sensor modalities in human detection applications instead of, or to complement, vision-based solutions for in-

creased robustness is still a relatively unexplored area of research.

Development of self-driving cars has also accelerated the development of terrain traversability analysis methods. However, the methods developed for self-driving cars are designed for structured environments and are not applicable off road in unstructured vegetated environments. Furthermore, estimating traversability in 3D requires also a 3D spatial model of the environment, which has high memory requirements. Consequently, despite some attempts to tackle the aforementioned issues, developing a large-scale 3D traversability map for unstructured vegetated off-road environments still remains a largely unsolved research challenge.

4. Methods Developed in the Thesis

This chapter summarizes the novel human detection and terrain traversability analysis methods this thesis proposed. First, Section 4.1 presents two separate human detection and tracking methods, described in more detail in Publication III and Publication IV. The first method exploits 2D LIDAR data, whereas the second method utilizes two different radar sensors. Second, Section 4.2 describes terrain traversability analysis and obstacle detection methods in unstructured natural environments. Subsection 4.2.1 describes a novel representation for 3D traversability analysis and two classification algorithms based on this representation capable of correctly classifying sparsely vegetated areas as traversable while still reliably detecting obstacles among the vegetation. Publication VII presents the details of this representation and the classification methods. Subsection 4.2.2 describes two approaches for augmenting LIDAR-based traversability maps with ultra-wideband (UWB) radar measurements to enhance the classification accuracy in densely vegetated environments. Publication V and Publication VI present these algorithms in detail.

4.1 Human Detection

Most of the existing human detection methods are based on vision solutions. A major drawback of these methods is that they are strongly affected by changes in illumination and do not operate in the dark. Therefore, this section presents two different human detection methods that take advantage of other sensor modalities, namely LIDAR and radar sensors. Thermal cameras are another sensor type immune to lighting conditions that are sometimes utilized in human detection applications. However, thermal cameras were not available in our research and are not discussed further in this chapter.

Table 4.1. Steps of the 2D LIDAR-based human detection and tracking algorithm

#	Algorithm steps
1.	Clustering a scan for human leg candidates
2.	Motion prediction and data association
3.	Human candidate update
4.	Leg classification and human candidate initialization
5.	Updating human existence probability

4.1.1 2D LIDAR-Based Human Detection

The basic idea of the 2D LIDAR-based human detection algorithm proposed in Publication IV is to detect and track human legs from each LIDAR scan and initialize a human candidate if the detected legs fulfill a set of predefined conditions. The human candidates are then tracked between consecutive scans and the human probability of a detected target being a human is constantly evaluated based on numerous features extracted from the LIDAR data. Table 4.1 lists the main steps of the algorithm and the following paragraphs explain these steps in more detail.

First, a LIDAR scan is segmented into clusters based on the Euclidean distance between neighboring measurements. Clusters with less than three data points are omitted from further processing due to insufficient information. Next, three informative features are extracted from all the remaining clusters: the size of cluster bounding box s, the circumference of the bounding box r, and the straightness of the cluster st. The straightness is defined as an average distance of the cluster points from the line between the first and last data point belonging to the cluster. Clusters fulfilling a set of predefined conditions are classified as human leg candidates.

All the segmented clusters are tracked and their motion is estimated based on their state in the previous step. A constant velocity model is used in the prediction step since it works well with frequent measurements. The predicted positions of the previously detected clusters are associated with the current detections, minimizing the distances between the corner points of the bounding boxes. This incorporates the comparison of the location and the cluster shape, which increases the robustness compared to the nearest neighbor data association scheme. After the

data association, the average of the cluster parameters (i.e., s, r, and st) for each cluster is updated with the latest data and stored for the classification step.

The motion of all human candidates is also estimated using the constant velocity model. The algorithm aims to associate a pair of leg candidates for each human candidate by evaluating the Euclidean distance between the leg and the human candidates. If suitable leg candidates are found, they are linked with a human candidate and removed from further processing.

The remaining clusters are classified with a leg classifier that compares the extracted features to predefined threshold values. The leg candidates are then paired up to form a pair with their closest other candidate. A new human candidate is initialized whenever the distance between a pair of legs is less than a predefined threshold value.

Finally, the human probability (probability of a human candidate to be a human) of each human candidate is updated based on a set of experimentally found informative features and coefficients. These features are the total traveled distance, the size of legs, the roundness of the legs, the distance between the legs, and the previous state of the human candidate. The classification is performed by comparing this value to an empirically discovered threshold value.

4.1.2 Radar-Based Human Detection

The main advantage of radars over most other sensors is that they are practically immune to adverse weather conditions and changes in the illumination. The angular resolution of radars is typically poor, however, when compared to other sensor modalities, and they provide little information of the target type. Publication III proposed a radar-based method to detect and track walking humans. The principle of this method is illustrated below.

The proposed method exploits data from two different radars: frequency modulated continuous wave (FMCW) radar operating at the millimeter band and a continuous wave Doppler radar operating at the K-band. The human detection and tracking are performed in three steps. First, human candidates are detected with the FMCW radar that returns a set of the strongest reflections perceived by the radar. Second, the human candidates are tracked with a Kalman filter-based, multi-target tracker. Third, the human probability of each candidate is updated based on the Doppler frequency's analysis and the estimated human candidates' speed.

The algorithm's first step is executed by the FMCW radar that performs signal processing for the raw sensor data and provides the following information about the strongest received reflections: distance, lateral distance from the center line, relative radial speed, relative radial acceleration, and variance of the lateral distance from the center line. At this stage, all the detected targets are considered as potential human candidates, since little information for classification is available.

In the second step, the detected targets are tracked with a multi-target tracker based on a Kalman filter. The human motion is modeled with the continuous Wiener process acceleration model can also handle sudden changes in target states. The data association problem is solved with the nearest neighbor (NN) method using the $1\text{-}\sigma$ uncertainty ellipses as the validation region. NN data association works well, because the tracked objects move relative slowly and the measurement frequency is high ($10\,Hz$).

The third step deals with updating the human probability of the human candidates. The human probability is updated separately from the Kalman filter with Bayes' formula based on information from both radars. Bayes' formula was a natural choice for updating the human probability conditional to the measured information, given the previous human probability. The velocity of each target is monitored based on the FMCW radar data and the vehicle motion information, and these estimated velocities are then compared with a human's average walking speed. This method is referred to as estimated velocity comparison (EVC). The human probability is increased when the velocity of a tracked target is around the average human walking speed and decreased in other cases. However, this approach incorporates a lot of uncertainty and the updates based only on the velocities are performed using conservative measurement probabilities with the Bayes' formula.

The Doppler radar is used to gain more evidence about the human candidates' class. The periodic motion of a walking human can be detected by analyzing the Fourier spectrogram of the Doppler frequency. This method is referred to as Doppler spectrum analysis (DSA). Figure 4.1(a) shows an example of a typical Doppler signature of a walking human, in which the signal's bandwidth varies periodically. Whenever this periodicity is observed, the human probability is updated with relatively high measurement probability.

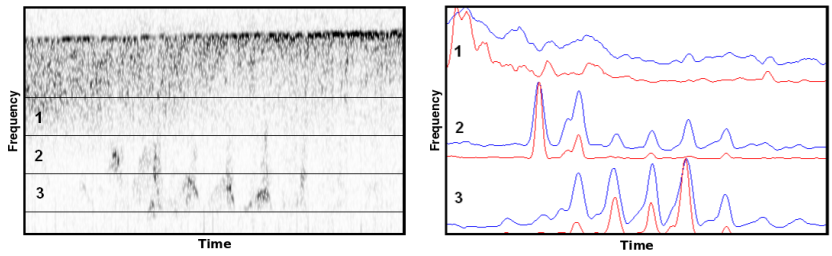

(a) (b)

Figure 4.1. (a) An excerpt of a spectrogram containing Doppler radar measurements of a walking human. The periodic motion can be seen on the bottom part of the spectrogram, which is divided into three bands that are analyzed separately. (b) The corresponding frequency mean (blue) and variance (red) of the three bands. The curves are normalized to the same scale. The three bands of the spectrogram and the corresponding frequency mean and variance are marked into the images with numbers 1, 2, and 3.

Detecting the periodic motion requires analysis of the signal's bandwidth, which can be measured by computing the signal's variance. However, there might be other frequencies in the spectrogram (e.g., moving vehicles), so it is necessary to analyze smaller bands of the frequency spectrum individually. Therefore, three slices of the spectrogram are analyzed in the proposed algorithm, and the frequency mean and variance of the slices are computed as a function of time. Figure 4.1(b) illustrates these signals computed from the spectrogram shown in Figure 4.1(a). The cadence frequency caused by the periodic motion is computed using the auto-difference function for all of these signals. Next, an Euclidean sum of squares is computed from these values to form one function. Furthermore, this function is normalized. Finally, we can determine the cycle length by finding the local minimum of the normalized function. Note that since the pace of a walking human is typically relatively low, the function needs to be observed for at least two seconds to form reliable classifications.

4.2 Terrain Traversability Analysis

This section introduces a compact 3D representation for estimating terrain traversability based on sensor data from unstructured off-road environments. It also introduces two novel traversability classification methods based on this representation that can classify sparse vegetation as traversable, while still reliably detecting the solid obstacles within the vegetation. Moreover, this section present two different approaches for

augmenting LIDAR-based traversability maps with UWB radar data to further improve the analysis accuracy in densely vegetated environments.

4.2.1 3D LIDAR-Based Traversability Classification

Publication VII refers to the new representation for 3D terrain traversability classification as Normal Distributions Transform Traversability Map (NDT-TM). NDT-TM builds on NDT Occupancy Map (NDT-OM) representation that divides the environment into voxels containing a normal distribution from the 3D points hitting a voxel. Contrary to traditional grid-based approaches, these cell distributions capture the inner structure of the cells, allowing the use of much larger cell sizes while retaining similar accuracy. NDT-TM incorporates three extra features — intensity mean, intensity variance, and permeability — for each cell that enable traversability classification in natural, unstructured environments. The proposed traversability classification methods classify the environment as traversable or non-traversable using a model learned with a support vector machine (SVM). The classification model is learned based on the following five features extracted from 3D LIDAR data: roughness, slope, permeability, intensity mean, and intensity variance, which are discussed in detail below. The proposed approach exploits automatic teaching example collection from semi-controlled environments, which completely removes the need for tedious hand-labeling.

Roughness R and inclination θ represent the environment geometry; they are computed based on the eigenvectors and eigenvalues of the cell distributions. The eigenvectors describe the principal components of a cell distribution; that is, a set of orthogonal vectors corresponding to the dominant directions of the covariance of the variables. The relationships between the corresponding eigenvalues define three different shapes for the cell distributions: spherical, linear, and planar. A cell distribution is spherical when all the eigenvalues are roughly equal, whereas one clearly larger or smaller eigenvalue compared to the other two indicate linear and planar cell distributions, respectively. Figure 4.2 illustrates the three different shapes of 3D normal distributions. The cell distributions are illustrated as 3-σ ellipsoids of the covariance matrix. The scaled eigenvectors are illustrated in the figure with red, green, and blue orthogonal lines.

Roughness R directly corresponds to the smallest eigenvalue of a cell distribution. That is, R captures the roundness of a distribution. For

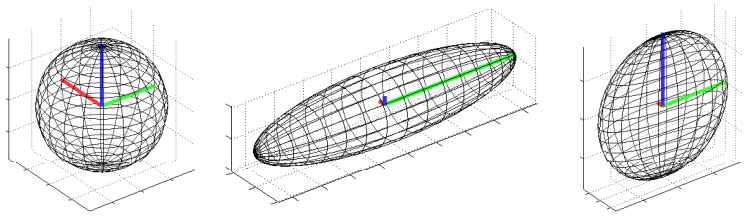

(a) Spherical (b) Linear (c) Planar

Figure 4.2. An illustration of different shapes of 3D normal distributions, depending on the relationships between the eigenvalues of the covariance matrix. The distributions are illustrated with ellipsoids that are 3-σ isosurfaces of the covariance matrices. The scaled eigenvectors are illustrated with orthogonal red, green, and blue lines representing the principal components of the distributions. (a) Spherical: all eigenvalues of the covariance matrix are approximately equal. (b) Linear: one eigenvalue is much larger than the others. (c) Planar: one eigenvalue is much smaller than the other two.

example, in case a cell distribution depicts a smooth surface, the smallest eigenvalue is much smaller than the other two eigenvalues; that is, R is low. Conversely, in the case of a spherical cell distribution, all the eigenvalues are roughly the same, which yields higher R. In other words, scattered measurements suggest that the cell distribution is rough and needs to be considered non-traversable.

Inclination θ is calculated by computing the angle between the eigenvector corresponding to the smallest eigenvalue and the vertical surface normal. The direction of the eigenvector is arbitrary with rough cells, and θ might not correspond to the inclination. However, with planar distributions, θ yields good estimates of the true inclination.

The remaining features capture properties specific for vegetation; that is, range measurements often penetrate vegetation contrary to solid obstacles. Additionally, chlorophyll, which is found in living plants, strongly reflects near-infrared (NIR) light but absorbs blue and red visible light.

Permeability ρ captures the probability of a LIDAR ray "passing through" a cell distribution rather than "hitting" it. That is, the hits and misses are computed for each cell by evaluating if the measurements hitting or passing through a voxel are statistically close enough to the cell distribution. See Publication VII for details on how to compute the hits and misses. The hits and misses need to be added to the environment model, since they are not stored by the NDT-OM representation by default. Note that LIDAR measurement hitting a voxel does not mean that it hits or passes through a cell distribution. Figure 4.3 illustrates the different cases of

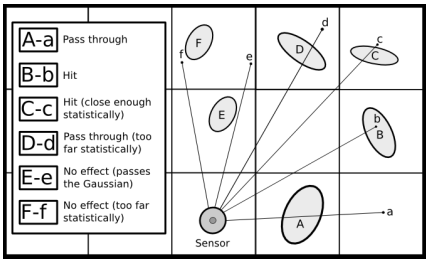

Figure 4.3. An illustration of different situations of a laser beam hitting an NDT cell.

LIDAR measurements hitting a voxel in a simplified 2D projection.

The reflectance of the environment is modeled with one-dimensional normal distribution, that is, the intensity mean μ_I and the intensity variance Σ_I. The intensity distribution is computed from all the measurements used to generate a cell distribution.

Terrain traversability depends on the aforementioned features, but it is not straightforward to determine the model between these features and the traversability. The key idea in the classification is to exploit the operator's ability to identify the terrain traversability. That is, the operator defines (labels) areas that are traversable and non-traversable and the selected features are extracted from the sensor data corresponding to these areas. Labeling these areas could be performed from the remote stations based only on transmitted data, but to guarantee good quality data, it is recommended that the operator has at least seen the areas on the spot. After this labeling process, these features have a class and can be used as an input for the machine learning algorithm, which eliminates the need for manually engineering classification model or adjusting thresholds.

The classification is based on the C-support vector classification (C-SVC) technique that requires teaching examples from both classes. It uses an automatic data collection scheme to avoid infeasible hand-labeling of the training examples. The positive samples are gathered from footprint points of a human-driven vehicle. The negative samples are gathered from a semi-controlled environment with relatively flat ground, assuming that all the cells above or below the ground plane are non-traversable. Clearly, not all of these cells are non-traversable; however, even training against an approximate labeling is enough to improve the overall performance.

Publication VII presents two different classification approaches. The first method performs C-SVC classification for all the cells in the map containing a cell distribution. Another approach is to first perform simple

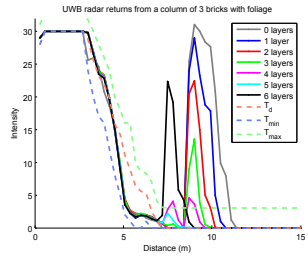

Figure 4.4. An example of the vegetation penetration capabilities of the UWB radar utilized in Publication V and Publication VI. In this experiment a column of three bricks is placed $9\,m$ away from the radar and vegetation is added layer by layer $1\,m$ in front of the brick column (see Publication V for details).

classification on all the cells using CTC that performs the classification based on only the roughness and inclination. The C-SVC classification is then performed only for the cells found non-traversable by the CTC method. The main advantages of this augmented CTC method (ACTC) is that it is computationally significantly lighter than the C-SVC method and captures the best properties from both classification methods.

4.2.2 Augmenting Traversability Maps with UWB Radar

Ultra-wideband (UWB) radars typically operate at relatively low frequencies and, therefore, can penetrate some amount of vegetation. Figure 4.4 illustrates the penetration capability of the UWB radar utilized in Publication V and Publication VI. The radar returns a vector of power measurements originating from objects within the field of view (FOV). The elements of this vector are referred to as range bins. In the figure, the radar return vectors are shown from an experiment, in which a column of three bricks was placed $9\,m$ away from the radar and vegetation was added layer by layer $1\,m$ in front of the brick column (see Publication V for details). The figure shows that the brick column can still be detected with four layers of vegetation (approximately $40\,cm$ thick). However, at this point the vegetation is already thick enough to result in a reflection similar to the brick column.

The studies in Publication V and Publication VI present two different methods for augmenting LIDAR-based traversability maps with UWB radar data such that areas of obstacle-free foliage can be cleared. The resulting augmented traversability maps capture the fine resolution of the LIDAR and the penetrating capabilities of the UWB radar.

Both of the presented methods follow three main steps. First, a traversability map is generated from the LIDAR data. Second, the UWB radar data is converted into occupancy probabilities using a custom sensor model. Third, the UWB radar detections are fused with the LIDAR-based traversability map. These steps are explained below in more detail.

A LIDAR-based traversability map can be generated using any available method, as long as the resulting map can be represented as a grid-based traversability map where each cell contains a continuous traversability index τ that is scaled such that $\tau \in [0,\ 1]$ (small τ means easy to traverse). In Publication V and Publication VI, the T-transform was applied for elevation maps as in Ye and Borenstein (2004). A 3D LIDAR needs to be utilized to perform the obstacle detection in real-time for constantly updating a local traversability maps while the vehicle is moving.

The second step requires processing of the UWB radar data. A sensor model is required to interpret the noisy UWB radar data. Only few studies exist in which a UWB radar is utilized as a part of a UGV sensor system; therefore, no out-of-the-box sensor models are available. The studies in Publication V and Publication VI present two different sensor models aimed particularly for UWB radar-based obstacle detection in vegetated environments.

A sensor model was developed and manually tuned in Publication V based on several experiments. The distinction between a target and a clear space is determined based on a threshold that is learned from data gathered while driving on obstacle-free terrain. The detection threshold is computed as a mean of the gathered measurements for all the range bins. The minimum and maximum values are also computed and utilized to determine the occupancy probabilities. The sensor model takes into account four main factors: the distance to the target, the angle to the target, the intensity of the radar return, and the shape of the radar return. Additionally, areas in the radar FOV after the detected targets are updated more conservatively due to the attenuation of the radar signal. Figure 4.5 shows an example of a radar return vector and the corresponding probabilities computed with the sensor model for the whole effective FOV of the radar. There are three targets present in the radar FOV in this example.

The work in Publication VI presents another sensor model whereby the whole sensor model is learned from experimental data, eliminating the need for hand-tuning the model's parameters. An SVM is exploited in

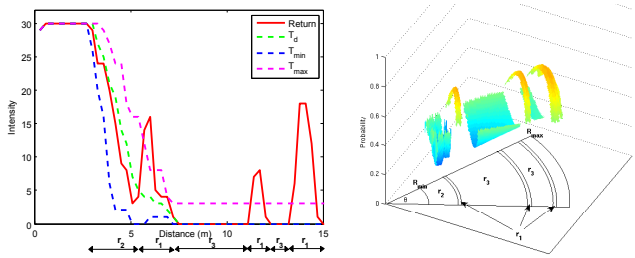

(a) (b)

Figure 4.5. (a) A UWB radar return vector with three targets in the FOV. The radar return vector is drawn with a red solid line, while the dashed lines represent the sensor model's detection thresholds (see Publication V for details). (b) Corresponding occupancy probabilities that are calculated with the sensor model for the whole FOV of the radar, assuming that all the targets are situated in the center of the FOV.

learning the sensor model. Thus, training the model requires labeled sensor data from positive and negative classes. The teaching data are gathered from a controlled environment where the object locations are known to simplify the labeling task. A LIDAR-based traversability map is first constructed from the environment, and representative examples from both classes are labeled on the map. Then, the features used in classification are extracted. The radar measurements are gathered at the same time as the LIDAR data used to generate the map are projected on the map based on vehicle pose and timestamp information, allowing the association of the labeled cells and the radar data. The features used for classification are the angle, the distance, and the corresponding measured intensity. The teaching data, preprocessed to ensure balanced and properly scaled data, are used to train the SVM. Since the desired output of the sensor model is occupancy probabilities, an SVM with the probability estimates extension is used. A separate model is trained for each range bin, since the separate models are much simpler than one complex model, which makes the prediction step significantly faster. Moreover, training more specified models enables better classification accuracy with limited training data. Applying the sensor model can be done by extracting the features of the interesting objects and inputting them to the learned model. However, in cases with multiple objects at the same range, the model does not perform correctly, since it assumes that the measured intensity originates from the object in question, while in reality the radar only return one intensity per range. Therefore, an angle scaler is applied to resolve these cases, which models the radar beam

pattern with an inverse parabola and scales the predicted probabilities accordingly, assuming that the measured intensity originates from an object closest to the center of the FOV.

The UWB radar detections are combined with the LIDAR-based maps after applying the sensor model in both publications. The LIDAR measurements are normally very accurate, and LIDAR-based ground plane detection is a reliable approach in open fields. However, LIDAR cannot see through vegetation and, therefore, cannot be used to predict the dense vegetation traversability. In contrast, the UWB radar measurements are very noisy, but the radar signal can penetrate vegetation. Therefore, only the cells seen as obstacles by the LIDAR are updated with the UWB radar. This way, the radar data are only used to gather more information about the objects detected by the LIDAR, and the noisy radar measurements do not generate false objects on the areas classified already traversable using the LIDAR data.

5. Results

Developing a functional unmanned ground vehicle (UGV) system for task-oriented operation is a demanding task. Describing the development process and system structure of such a system is one of the contributions of this thesis. Since fully autonomous task execution in unstructured environments is not yet practical, scalable level of autonomy is needed to support the UGV operator. However, one important observation from developing the UGV demonstrator (see Section 2.4) was the apparent need for automatic methods for human detection and traversability analysis to improve the UGV usability and safety. Several novel algorithms were developed in an attempt to solve these shortcomings that address these issues. Chapter 4 summarized the novel human detection and terrain traversability analysis methods this thesis proposed, whereas this chapter provides the most important results that validate these method's performance. Refer to the articles of this thesis for a full evaluation of the methods.

5.1 Human Detection

This section presents the essential results from the field experiments performed for evaluating the human detection methods proposed in Publication III and Publication IV.

5.1.1 2D LIDAR-Based Human Detection

Four different experiments were conducted to validate the performance of the 2D LIDAR-based human detection algorithm presented in Publication IV. The measurement platform was moving in a typical office environment, while one target person was moving in the LIDAR field of view (FOV) during the whole of the experiments. The target person wore dif-

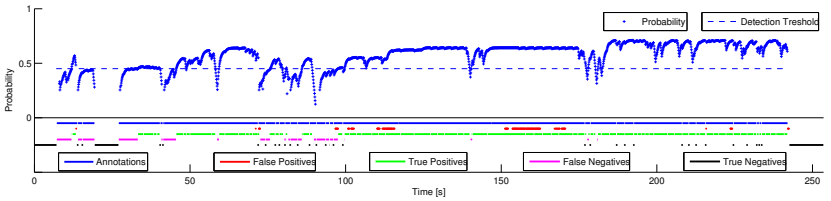

Figure 5.1. The 2D LIDAR-based human detection algorithm's performance in the first experiment. The blue crosses represent the human candidates initiated by the algorithm and the blue dashed line marks the human classification threshold. On the bottom of the figure, the green line illustrates the annotated target persons during the experiment. The red, blue, magenta, and black lines denote the false positive (FP), true positive (TP), false negative (FN), and true negative (TN) observations respectively.

ferent clothing in the experiments. The target person was wearing regular dark trousers in the first experiment, whereas the target person was wearing jeans, shorts, and white trousers in experiments 2 – 4, respectively. Additionally, there are a few random people passing by during the experiments 2 – 4. Each experiment lasted around four minutes. The test data were annotated frame-by-frame by a human expert for evaluation purposes.

Figure 5.1 illustrates the algorithm performance in the first experiment, where only one human was present in the radar FOV. The blue crosses represent human candidates generated by the algorithm, and the blue dashed line is the empirically derived human classification threshold. That is, when the human probability rises over the line, the human candidates are confirmed as humans. The bottom part of the figure shows the annotations and the true and false detections by the proposed human detection algorithm.

Table 5.1 further demonstrates the algorithm's performance in all the experiments. The first line shows the mean errors of the detections with respect to the annotations, while the second line denotes the corresponding standard deviations. The third and fourth lines show the true positive rates and the accuracies, respectively. The true positive rate is the ratio of TP over the sum of TP and FP, whereas the accuracy is the ratio of the sum of TP and TN over the sum of TP, FN, TN, and FP.

5.1.2 Radar-Based Human Detection

The performance of the radar-based human detection method was evaluated in two different environments. The first experiment was performed in a mine with only one person present in the sensor system's FOV. The

Table 5.1. Performance of the 2D LIDAR-based human detection algorithm

	Regular	Jeans	Shorts	Light
Mean error $[m]$	0.0327	0.0360	0.0267	0.0284
Standard deviation $[m]$	0.0314	0.0372	0.0369	0.0369
True positive rate $[\%]$	82.8	87.5	81.5	85.8
Accuracy $[\%]$	77.3	77.8	67.6	72.5

second experiment was conducted in a harbor environment, where two persons were simultaneously walking in the FOV. The measurement platform was stationary in both experiments. Additional experiments were performed with moving platform; however, it was discovered that the motion induced strong signals into the Doppler spectrum that effectively masked the Doppler signature of walking humans.

Figure 5.2 illustrates the performance of the radar-based human detection algorithm. The trajectories of the people moving in the FOV are illustrated in the figures with differently colored dots. The black dots indicate that the person is detected but not classified as human, whereas the red dots represent people who are classified as humans. The gray dots represent positions where human targets were not observed with the radar measurement system. Moreover, the blue dots are radar measurements originating from other objects or clutter measurements.

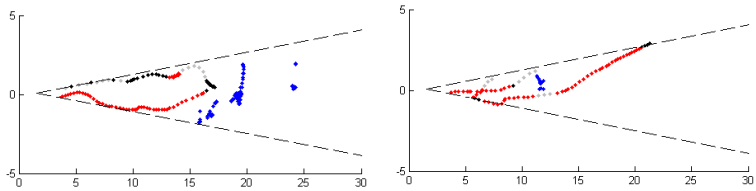

(a) (b)

Figure 5.2. (a) Results from the experiment in a mine environment. (b) Results from the experiment in a harbor environment.

Table 5.2 summarizes the relevant information from Figures 5.2(a) and 5.2(b). The first column shows the human target detection percentage. These detections are tracked by the sensor system but are not necessarily classified as humans. The second column shows the percentage of targets classified as humans using only EVC method, whereas the third column contains the classification percentages using both EVC and DSA methods.

Table 5.2. Radar-based human detection method performance

	Detected	Classified (EVC)	Classified (EVC+DSA)
Mine	89.89%	32.58%	55.06%
Harbour	83.16%	0%	78.95%

5.2 Terrain Traversability Analysis

This section presents the relevant results from the experiments performed to validate the terrain traversability analysis methods proposed in Publication V, Publication VI, and Publication VII.

5.2.1 3D LIDAR-Based Traversability Classification

Section 4.2.1 presented two different traversability classification methods for exploiting the novel Normal Distributions Transform Traversability Map (NDT-TM) representation. These methods were validated using data from five different environments. The experiments were performed on asphalt, gravel, sparse grass, dense grass, and in a forest environment. To ensure the correct classification of the obstacles, five obstacles were placed in known locations on the densely vegetated field within vegetation that were all correctly classified by the proposed traversability classification methods. The measurement platform was moving extensively around the environment in all the experiments to ensure comprehensive mapping of the environment.

Table 5.3 summarizes the performance of the two proposed classification approaches, i.e., C-support vector classification (C-SVC) and augmented CTC (ACTC), from the first four experiments compared to the constant threshold classifier (CTC) method. The same numbers could not be computed from the forest environments, since the ground truth was unknown. The recall is defined as the ratio of TP over the sum of TP and FN, the precision is the ratio of TP over the sum of TP and FP. The f-score is computed twice the product of precision and recall over the sum of precision and recall.

The final experiment was performed in a forest environment with sparse grass and multiple coniferous and deciduous trees spread across the environment. The experiment was performed with a different measurement platform, and no data from forest environments were used to train our model. Therefore, this experiment illustrates that the trained model gen-

Table 5.3. Classification results of the LIDAR-only 3D traversability analysis

	Precision	Recall	f-score
Trial 1: Asphalt			
CTC	**0.9703**	**0.9983**	**0.9841**
C-SVC	0.9691	**0.9983**	0.9835
ACTC	0.9691	**0.9983**	0.9835
Trial 2: Gravel			
CTC	**0.8709**	0.9784	**0.9215**
C-SVC	0.8525	0.9953	0.9184
ACTC	0.8476	**0.9979**	0.9166
Trial 3: Sparse grass			
CTC	**0.9810**	0.9017	0.9397
C-SVC	0.9787	0.9490	**0.9636**
ACTC	0.9735	**0.9502**	0.9617
Trial 4: Dense grass			
CTC	0.9755	0.6175	0.7563
C-SVC	**0.9855**	0.6977	0.8170
ACTC	0.9822	**0.7113**	**0.8250**

eralizes well to different environments. Figure 5.3 shows top-down views of maps generated from the environment. From left to right, the maps are NDT Occupancy Map (NDT-OM) colorized by height, NDT-TM classified with CTC, and NDT-TM classified with ACTC. No cells above the sensor level are visualized to make the visualization of the NDT-TMs more clear. The white dotted line in the NDT-OM illustrates the vehicle trajectory during the data gathering, and the black circles in the NDT-TM maps mark locations of tree trunks along the trajectory. The black rectangles highlight areas with tall grass where the classification methods perform differently.

Both the CTC and ACTC methods correctly classified all tree trunks as non-traversable. However, some areas with tall grass are misclassified with the CTC, whereas the ACTC was able to correctly classify the whole area; that is, using the ACTC method for classification enables safe path planning in the forest environment even with tall sparse grass. Most of the non-traversable areas in the maps near tree trunks originate from low-hanging tree branches that should not be considered traversable, since the branches might hit and damage the sensor.

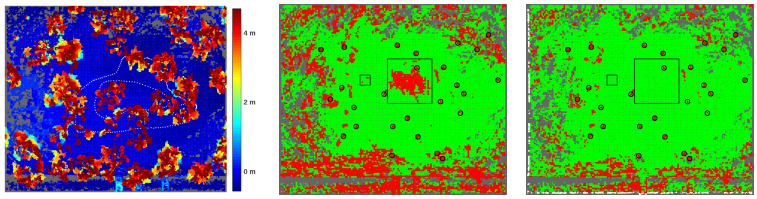

(a) NDT-OM (b) NDT-TM: CTC (c) NDT-TM: ACTC

Figure 5.3. Top down view of the resulting maps from the forest experiment. The size of the test area is $60 \times 50\,m^2$. (a) NDT-OM map of the forest environment color-coded based on height. The white dotted line illustrates the trajectory of the measurement platform. (b) NDT-TM map of the forest environment classified with the CTC method. (c) NDT-TM map classified with the ACTC method. The black circles mark locations of tree trunks along the measurement platform trajectory. The black rectangles highlight areas where sparse vegetation is misclassified with the CTC method, while the ACTC methods correctly classify the area as traversable. The NDT-TM maps are truncated to present only cells lower than the sensor height for clarity.

5.2.2 Augmenting Traversability Maps with UWB Radar

Both of the methods proposed in Publication V and Publication VI were validated using data from the same two field trials. The first trial was performed in a controlled environment in which three obstacles were placed on the field, and branches of an ash tree were added layer by layer in front of the obstacles, as well as on two clear areas. Each new layer added approximately $10\,cm$ of vegetation. The measurement platform was driven within the field such that all the obstacles were within the FOV of the measurement system. The second experiment was conducted in a rural environment with multiple grass tufts on the experiment area. Additionally, three brick piles (heights: 2, 3, and 4 bricks) were placed in the area. Furthermore, there is a passenger car and a ditch on the test site. Again, the measurement platform was maneuvered such that all the objects were visible for the sensor system.

Table 5.4 summarizes the performance of both of the proposed methods from the first experiment. The table rows illustrate the performance with different amounts of vegetation present. In the table, the best results (i.e., highest true negative rate (TNR) and the lowest false negative rate (FNR)) are shown in bold font. Similar values from the second experiment cannot be computed, since the ground truth is unknown.

Figure 5.4 illustrates the performance of the algorithm in the second trial. Figure 5.4(a) shows the traversability map of the test site computed only based on the LIDAR measurement. Figure 5.4(b) illustrates the

Table 5.4. Performance of the traversability analysis using UWB radar

	Learned model		Handcrafted model	
	TNR	FNR	TNR	FNR
a) Empty	N/A	**6.67%**	N/A	6.81%
b) Obstacles	N/A	**12.68%**	N/A	15.42%
c) 1 layer	**92.40%**	9.01%	88.98%	**8.59%**
d) 2 layers	**92.86%**	**14.21%**	88.49%	17.60%
e) 3 layers	**83.96%**	**12.25%**	75.00%	13.87%
f) 4 layers	**83.09%**	14.85%	65.69%	**10.37%**

measurement platform trajectory, in which the cells observed with the UWB radar are shown with an intensity of gray proportional to the time spent by the cell in the radar FOV. A darker color indicates longer time in the FOV. Figures 5.4(c) and 5.4(d) show the augmented traversability maps using both of the proposed methods.

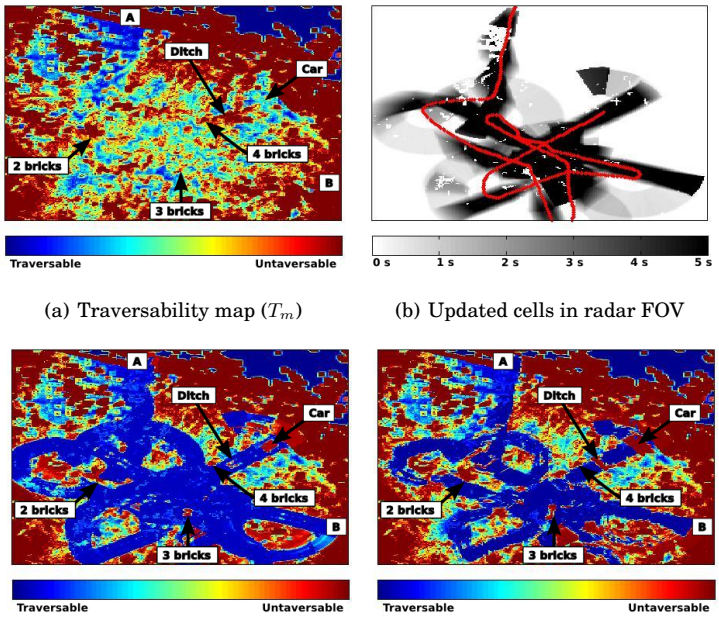

(a) Traversability map (T_m)

(b) Updated cells in radar FOV

(c) T_{ma} using learned sensor model

(d) T_{ma} using handcrafted model

Figure 5.4. Rural experiment: (a) shows the LIDAR traversability map, colored by traversability value (red means obstacle); (b) shows the cells that were observed by the radar, with an intensity of grey proportional to the time spent by the cell in the radar FOV (darker means longer time), and the UGV trajectory shows with red dots; (c) shows the augmented occupancy map using the learned sensor model, colored by the probability value (blue for 0, red for 1). (d) shows the augmented occupancy map using a handcrafted sensor model, colored by the probability values. The size of the test area is around $50 \times 50\,m^2$.

6. Discussion

This thesis proposed novel methods that enable enhancing the navigation performance of unmanned ground vehicles (UGVs) operating in unstructured natural environments. This chapter further discusses the proposed methods and the presented results from the validation experiments.

6.1 Human Detection

The main advantage of the 2D LIDAR-based human detection method summarized in Section 4.1.1 is that it is computationally very light and can be deployed in systems with limited computational capacity. The algorithm performs well for both stationary and mobile platforms and can detect and track multiple humans simultaneously. The results illustrate that the tracking accuracy is good, as the mean error from the manually annotated ground truth averages around $3\,cm$. The classification performance could still be improved, as the true positive rate from all the experiments averages around 85% and the accuracy averages around 75%. One direction of future work is to utilize a suitable optimization method to select the free parameters in the proposed method.

Nonetheless, the main reason for the seemingly low classification accuracy is that it takes some time to accumulate evidence about the target classes when using only 2D LIDAR data for the classification. That is, fast moving people can leave the field of view (FOV) before they are classified as humans. However, these people do not remain unnoticed. They are interpreted as objects from the sensor data but not yet classified as humans. A simple way to increase the classification accuracy would be to add other sensor modalities, such as a vision sensor to provide more evidence about the target classes.

Data fusion would also be beneficial when operating outdoors under dynamically changing environmental conditions, since 2D LIDARs provide insufficient information for reliable human detection under adverse weather conditions in complex outdoor environments. Therefore, enabling operation in such environments requires augmenting the proposed 2D LIDAR-based human detection method with other sensor modalities (e.g., 3D LIDAR, vision sensor, radar) to guarantee detection within the available time frame. However, this would require extensive testing under different environmental conditions and is left as future work.

The radar-based human detection method recapitulated in Section 4.1.2 demonstrated that walking people can be classified and tracked using only radar technology. The results show that targets can be detected with the utilized radar equipment around nine times out of ten when new data are received. Nonetheless, the frequency modulated continuous wave (FMCW) radar has a relatively narrow FOV, and most of the targets that remain undetected reside at the edges of the radar FOV where the signal is much weaker. Using a radar with a wider FOV would increase the detection accuracy (assuming that the FOV edges would be avoided). The target classification accuracy based only on the estimated velocity comparison is low, as expected. When incorporating processed information from the Doppler radar, the classification accuracy arises significantly, averaging 67% between both experiments. The percentage is not high enough for this method to be used as a stand-alone human detection method for UGVs, but it demonstrates that Doppler radar provides valuable information about moving people.

Doppler radar measures motion components that are directed towards or away from the radar. Therefore, the Doppler radar cannot detect people who are stationary or walking straight across the radar FOV. Furthermore, in contrast to most radars, Doppler radar data are affected by rain, since the movement of rain droplets cause noise to the Doppler spectrum. Additionally, sensor system's movement affects the Doppler spectrum. Nonetheless, if the environment does not containing any strong radar reflectors, Doppler radar can also be used while the radar is moving. The relative velocities of walking people will change, but walking people can still be detected, because the proposed algorithm only observes the periodicity of the motion. They can be falsely classified as humans in the presence of other moving targets, especially if there is already a walking human in the FOV. That is, the measured Doppler spectrum cannot be

associated with the correct target with the current sensor setup.

FMCW radars and Doppler radars exploit the same phenomena by measuring the frequency shift between transmitted and received signal. The FMCW radar utilized in the study also measures the Doppler frequency internally. Therefore, if the raw sensor data were available, it should be possible to implement the proposed algorithm using only the FMCW radar. This would enable the system to distinguish Doppler signatures caused by different people, since the Doppler signatures would be centered on the frequency respective to the distance measured with the FMCW principle.

The fundamental objective of developing human detection algorithms for UGVs is to relieve human operators from monitoring the environment, thus allowing them to concentrate on higher-level task execution. Therefore, in addition to the performance metrics discussed earlier, the algorithm performance should also be compared to the performance level achieved by human operators. State-of-the-art human detection methods presently provide impressive performance but cannot yet guarantee better performance than human operators, since people are particularly good at comprehending the environment they perceive. An experienced and focused human operator can detect practically all people (even partially visible) in clear visibility without false positives.

However, human operators have a limited FOV and occasionally tend to loose concentration. Automation eliminates human errors and enables uninterrupted operation. Moreover, it is possible to create a more complete model of the surrounding environment using sensor data, as all sides of a UGV can be observed simultaneously using multiple sensors. Additionally, various sensors see in the dark whereas some sensors even see through obstacles. Therefore, the constantly developing technology promises superhuman human detection performance already in the near future. Nonetheless, it will take much longer before UGVs can operate in unstructured and populated environments without any human supervision.

6.2 LIDAR-Based Traversability Analysis

Section 4.2.1 summarized the Normal Distributions Transform Traversability Map (NDT-TM) representation for traversability analysis and the proposed traversability classification methods utilizing this novel repre-

sentation. The presented results illustrate that the two proposed methods perform equally well compared to the previous work in simple environments, but they improve the traversability classification results significantly in unstructured natural environments. That is, by exploiting the permeability and intensity distribution, it is possible to improve the traversability classification accuracy and still distinguish solid, partially visible obstacles within vegetation.

The proposed traversability classification methods are based on a support vector machine (SVM) that is trained with automatically collected training samples. However, while the positive samples are gathered from the UGV footprint ensuring good quality samples, the negative samples are collected from a semi-controlled environment using a rough approximate method, which results in a lower quality negative example set. Therefore, to avoid the approximative collection of negative samples, preliminary experiments were also performed with one-class SVM algorithm (Schölkopf et al., 2001), whereby only positive samples are used to train the model. However, tuning a one-class SVM is difficult without labeled data from both classes. Therefore, when training the one-class SVM, selecting the parameters was performed similarly as with the C-SVC approach; that is, by running cross validation on the same labeled validation data. Nonetheless, even the models tuned using validation data with labeled samples from both classes performed systematically significantly worse than the two-class models. Further investigation into one-class classifiers is left as one direction of future work.

One key finding of the study was that, even though NDT Occupancy Map (NDT-OM) allows low resolution without compromising model accuracy, it is beneficial to keep the voxel size in NDT-TM relatively small to capture the real dimensions and properties of the environment in order to correctly classify vegetated environments. However, significantly lower resolutions than in previous work can still be utilized. The computational efficiency of NDT-TM-based classification could be further improved by utilizing a multi-resolution framework as a basis of the NDT-TM mapping, which would allow reasonably small resolution for classifying sparse vegetation in places of interest and large grid size in areas with little or no data. However, this is left as future work. Moreover, the NDT-TM provides a solid foundation for traversability classification that could be further improved by adding other sensor modalities. For example, UWB radar measurements, which have been shown to penetrate vegetation,

could be incorporated into the representation, enabling safe navigation performance even in densely vegetated environments.

6.3 Augmented Traversability Maps

The methods summarized in Section 4.2.2 augment traversability maps with UWB radar data. UWB radars can penetrate vegetation and, therefore, are a valuable addition to UGV sensor systems. However, there are only a few radars on the market, which is probably the main reason that UWB radars are seldom utilized in UGV systems. Nonetheless, the results presented in Publication V and Publication VI are extremely encouraging and demonstrate that UWB radars are remarkably beneficial when operating in vegetated environments. With the proposed method, more than 80% of obstacle-free foliage can be removed while still detecting solid obstacles, even if there are around $40\,cm$ of foliage in front of the obstacles.

However, the radar utilized in the experiments is very noisy and, based on the data, it is impossible to distinguish targets with a small radar cross-section, which may lead to ignoring small difficulties in the terrain detected by the LIDAR when utilizing the proposed methods. Even if these targets are typically not a significant threat to robot's integrity, it is still preferable to detect them to anticipate any difficulty (e.g., to reduce the UGV's speed).

The developed methods are applicable to various environments with different types of vegetation. However, the amount of cleared, obstacle-free vegetation may depend on the type of vegetation. For example, wet grass or vegetation with a high concentration of branches will result in stronger backscattering of the radar signal; that is, less obstacle-free vegetation can be cleared.

To further improve the performance, in future work, the radar should be mounted on a scanning mechanism (e.g., pan-tilt unit) or use an overlapping array of radars, which would enhance the accuracy of the collected radar data, as well as the augmented traversability map. Furthermore, the validation results were obtained off-line; however, no heavy computations are involved in the process. Therefore, using a 3D LIDAR to update a local traversability map (e.g., NDT-TM) continuously should also enable continuous real-time update of the local augmented 3D traversability map.

7. Conclusions

The main objective of this thesis was to develop novel methods enabling safe off-road navigation for UGVs in unstructured natural environments. The whole chain of developing an off-road capable UGV was studied, and Publication II presents the mechatronics design of such a vehicle. However, the main focus of this thesis was on developing innovative methods for enhancing the navigation performance in off-road environments that are achievable with current state-of-the-art methods.

This thesis particularly proposed new methods for traversability mapping and analysis in vegetated environments. A new, efficient 3D representation for traversability mapping, i.e., Normal Distributions Transform Traversability Map (NDT-TM), was introduced that can be utilized in large-scale traversability analysis in unstructured natural environments. Additionally, two methods were proposed for traversability classification exploiting NDT-TM representation that outperform the previous work in unstructured environments. Moreover, this thesis presented two innovative approaches for augmenting LIDAR-based traversability maps with ultra-wideband (UWB) radar data. Since UWB radars can penetrate vegetation, applying these methods for augmenting traversbility maps enables clearing most of the obstacle-free vegetation from traversability maps. In other words, these methods enable safe navigation performance for UGVs even in densely vegetated environments.

Furthermore, two new methods were proposed for human detection using alternative sensor modalities to vision sensors. The developed human detection methods take advantage of LIDAR and radar data instead of traditionally used image data. The first method only exploits 2D LIDAR data, whereas the other method relies only on radar data. The LIDAR-based human detection method is computationally very light and can be executed on systems with limited computational capacity.

The other developed human detection method only exploits radar data, making it more robust against adverse weather conditions. Although promising results were achieved with the developed methods, these techniques should be further combined with other sensor modalities to increase robustness and accuracy when operating in unstructured outdoor environments. However, fusing detections from other sensor modalities should be straightforward by using, for example, model-based sensor fusion techniques, such as the Kalman filtering exploited in Publication III.

The proposed methods were implemented on several separate platforms and, therefore, this thesis did not present experiments using a UGV running all the proposed algorithms at once, which is left as future work. However, all the developed methods were validated using real UGV systems and showed promising results in the extensive experiments. Thus, by exploiting the methods presented in this thesis, it should be feasible to develop a UGV able to navigate safely within densely vegetated populated environments.

References

Ackerman, E. (2014). Korean competition shows weather still a challenge for autonomous cars. *IEEE Spectrum*. 11 November.

Amidi, O. (1990). Integrated mobile robot control. Technical Report CMU-RI-TR-90-17, Robotics Institute, Carnegie Mellon University, Pittsburgh, PA.

Angelova, A., Matthies, L., Helmick, D., and Perona, P. (2007). Fast terrain classification using variable-length representation for autonomous navigation. In *Proceedings of the IEEE Conference on Computer Vision and Pattern Recognition (CVPR)*, Minneapolis, MN, USA.

Arras, K., Grzonka, S., Luber, M., and Burgard, W. (2008). Efficient people tracking in laser range data using a multi-hypothesis leg-tracker with adaptive occlusion probabilities. In *Proceedings of the IEEE International Conference on Robotics and Automation (ICRA)*, pages 1710–1715, Pasadena, CA, USA.

Arras, K., Mozos, O., and Burgard, W. (2007). Using boosted features for the detection of people in 2D range data. In *Proceedings of the IEEE International Conference on Robotics and Automation (ICRA)*, pages 3402–3407, Roma, Italy.

Arras, K. O., Lau, B., Grzonka, S., Luber, M., Mozos, O. M., Meyer-Delius, D., and Burgard, W. (2012). Range-based people detection and tracking for socially enabled service robots. In *Towards Service Robots for Everyday Environments*, volume 76 of *Springer Tracts in Advanced Robotics*, pages 235–280.

Bacha, A., Bauman, C., Faruque, R., Fleming, M., Terwelp, C., Reinholtz, C., Hong, D., Wicks, A., Alberi, T., Anderson, D., Cacciola, S., Currier, P., Dalton, A., Farmer, J., Hurdus, J., Kimmel, S., King, P., Taylor, A., Covern, D. V., and Webster, M. (2008). Odin: Team VictorTango's entry in the DARPA Urban Challenge. *Journal of Field Robotics*, 25(8):467–492.

Bagnell, J. A., Bradley, D., Silver, D., Sofman, B., and Stentz, A. (2010). Learning for autonomous navigation. *IEEE Robotics Automation Magazine*, 17(2):74–84.

Bajracharya, M., Howard, A., Matthies, L., Tang, B., and Turmon, M. (2009). Autonomous off-road navigation with end-to-end learning for the LAGR program. *Journal of Field Robotics*, 26(1):3–25.

Bajracharya, M., Ma, J., Malchano, M., Perkins, A., Rizzi, A., and Matthies, L. (2013). High fidelity day/night stereo mapping with vegetation and negative obstacle detection for vision-in-the-loop walking. In *Proceedings of*

the IEEE/RSJ International Conference on Intelligent Robots and Systems (IROS), pages 3663–3670, Tokyo, Japan.

Bares, J., Hebert, M., Kanade, T., Krotkov, E., Mitchell, T., Simmons, R., and Whittaker, W. (1989). Ambler: an autonomous rover for planetary exploration. *IEEE Computer*, 22(6):18–26.

Bares, J., McFadden, S., Stentz, A., Richards, C., and Murray, S. (2002). Designing crash-survivable unmanned vehicles. In *Proceedings of the AUVSI Unmanned Systems 2002 Conference*, Lake Buena Vista, FL, USA.

Bares, J. and Stager, D. (2004). Expanded field testing results from Spinner, a high mobility hybrid UGCV. In *Proceedings of the AUVSI Unmanned Systems 2004 Conference*, Anaheim, CA, USA.

Bedord, L. (2016). Fully autonomous vehicles are coming. *Successful Farming*. 19 April.

Benenson, R., Omran, M., Hosang, J., and Schiele, B. (2014). Ten years of pedestrian detection, what have we learned? In *Proceedings of the European Conference on Computer Vision (ECCV), Workshop on Computer Vision for Road Scene Understanding and Autonomous Driving*, pages 613–627, Zürich, Switzerland.

Bertozzi, M., Broggi, A., Coati, A., and Fedriga, R. (2013). A 13,000 km intercontinental trip with driverless vehicles: The VIAC experiment. *Intelligent Transportation Systems Magazine, IEEE*, 5(1):28–41.

Biber, P. and Strasser, W. (2003). The normal distributions transform: A new approach to laser scan matching. In *Proceedings of the IEEE/RSJ International Conference on Intelligent Robots and Systems (IROS)*, volume 3, pages 2743–2748, Las Vegas, NV, USA.

Billingsley, J., Visala, A., and Dunn, M. (2008). Robotics in agriculture and forestry. In *Springer Handbook of Robotics*, Springer Tracts in Advanced Robotics, pages 1065–1077. Springer, Berlin, Heidelberg.

Bogue, R. (2016). Robots poised to revolutionise agriculture. *Industrial Robot: An International Journal*, 43(5):450–456.

Bohlmann, K., Beck-Greinwald, A., Buck, S., Marks, H., and Zell, A. (2013). Autonomous person following with 3D LIDAR in outdoor environments. *Journal of Automation, Mobile Robotics and Intelligent Systems*, 7(2):24–29.

Bohren, J., Foote, T., Keller, J., Kushleyev, A., Lee, D., Stewart, A., Vernaza, P., Derenick, J., Spletzer, J., and Satterfield, B. (2008). Little Ben: The Ben Franklin Racing Team's entry in the 2007 DARPA Urban Challenge. *Journal of Field Robotics*, 25(9):598–614.

Boston Dynamics (2013). Boston Dynamics: Dedicated to the Science and Art of How Things Move. `http://www.bostondynamics.com/index.html`. Accessed: 19.03.2016.

Boyd, J. (2015). Japan's plan to speed self-driving cars. *IEEE Spectrum*. 17 November.

Bradley, D., Thayer, S., Stentz, A., and Rander, P. (2004). Vegetation detection for mobile robot navigation. Technical Report CMU-RI-TR-04-12, Robotics Institute, Carnegie Mellon University, Pittsburgh, PA, USA.

Braid, D., Broggi, A., and Schmiedel, G. (2006). The TerraMax autonomous vehicle. *Journal of Field Robotics*, 23(9):693–708.

Buehler, M., Iagnemma, K., and Singh, S. (2008). Editorial. *Journal of Field Robotics*, 25(8):423–424.

Burgess, M. (2015). Formula E announces 300 kph "RoboRace" championship. *Wired*. 27 November.

Burgess, M. (2016). This car is the future of autonomous racing. *Wired*. 30 March.

Carnegie Mellon Media Relations (2006). Carnegie Mellon's National Robotics Engineering Center unveils futuristic unmanned ground combat vehicles. Press release. 26 April.

Carrier, D. (1992). Soviet rover systems. In *Proceedings of the AIAA Space Programs and Technologies Conference*, Huntsville, AL, USA.

Castano, A. and Matthies, L. (2003). Foliage discrimination using a rotating ladar. In *Proceedings of the IEEE International Conference on Robotics and Automation (ICRA)*, volume 1, Taipei, Taiwan.

Chang, T., Legowik, S., and Abrams, M. (1999). Concealment and obstacle detection for autonomous driving. In *Proceedings of the IASTED Conference on Robotics and Applications*, pages 28–30, Santa Barbara, CA, USA.

Chu, J. (2015). MIT Cheetah robot lands the running jump. *MIT News*. `http://news.mit.edu/2015/cheetah-robot-lands-running-jump-0529`.

Chung, W., Kim, H., Yoo, Y., Moon, C.-B., and Park, J. (2012). Detection and following of human legs through inductive approaches for a mobile robot with a single laser range finder. *IEEE Transactions on industrial electronics*, 59(8):3156–3166.

Connor, A. (2015). Semi-autonomous cars bring the self-driving car closer to reality. *Gear Patrol*. 23 October.

Cunningham, C., Wong, U., Peterson, K., and Whittaker, W. (2015). Predicting terrain traversability from thermal diffusivity. In Mejias, L., Corke, P., and Roberts, J., editors, *Field and Service Robotics*, volume 105 of *Springer Tracts in Advanced Robotics*, pages 61–74. Springer International Publishing.

Czapla, T. and Wrona, J. (2013). Technology development of military applications of unmanned ground vehicles. In Nawrat, A. and Kuś, Z., editors, *Vision Based Systemsfor UAV Applications*, volume 481 of *Studies in Computational Intelligence*, pages 293–309. Springer International Publishing.

Davies, A. (2015). Baidu's self-driving car has hit the road. *Wired*. 9 December.

Davies, A. (2016). Uber's Self-Driving Truck Makes Its First Delivery: 50,000 Beers. *Wired*. 25 October.

Dickmanns, E. (1997). Vehicles capable of dynamic vision. In *Proceedings of International Joint Conference on Artificial Intelligence*, pages 1577–1592, Nagoya, Japan.

Dickmanns, E., Mysliwetz, B., and Christians, T. (1990). An integrated spatio-temporal approach to automatic visual guidance of autonomous vehicles. *IEEE Transactions on Systems, Man and Cybernetics*, 20(6):1273–1284.

Dorains, G. A., Bonasso, R. P., Kortenkamp, D., Pell, B., and Schreckenghost, D. (1998). Adjustable autonomy for human-centered autonomous systems. In *Proceedings of the First International Conference of the Mars Scociety*, pages 397–420.

ELROB (2016). ELROB - The European Land Robot Trial. `http://www.elrob.org/`. Accessed: 19.03.2016.

Etherington, D. (2016). Baidu gets approval to test self-driving cars in California. *TechCrunch*. 31 August.

Eurathlon (2015). Robotic Competition - Eurathlon 2015. `http://www.elrob.org/eurathlon-2015`. Accessed: 19.03.2016.

G-NIUS (2016). Guardium MK I - G-Nius. `http://g-nius.co.il/unmanned-ground-systems/guardium-ugv.html`. Accessed: 06.03.2016.

Gage, D. (1995). UGV history 101: A brief history of unmanned ground vehicle (UGV) development efforts. *Unmanned Systems Magazine*, 13(3):9–16.

Garrido, S., Malfaz, M., and Blanco, D. (2013). Application of the fast marching method for outdoor motion planning in robotics. *Robotics and Autonomous System*, 61(2):106–114.

Gerónimo, D. and López, A. M. (2014). *Vision-based pedestrian protection systems for intelligent vehicles*. Springer, New York, NY, USA.

Google (2016). Google Self-Driving Car Project, Monthly Report (February). `https://static.googleusercontent.com/media/www.google.com/fi//selfdrivingcar/files/reports/report-0216.pdf`. Accessed: 04.03.2016.

Gürbüz, S., Melvin, W., and Williams, D. (2007). Detection and identification of human targets in radar data. In Kadar, I., editor, *Proceedings of the SPIE Signal Processing, Sensor Fusion, and Target Recognition XVI*, volume 6567, Orlando, FL, USA.

Hadsell, R., Bagnell, J., Huber, D., and Hebert, M. (2010). Space-carving kernels for accurate rough terrain estimation. *International Journal of Robotics Research*, 29(8):981–996.

Halme, A. and Koskinen, K. (1993). An approach to automate mobility of working machines in outdoor environment - the PANORAMA project. In *Proceedings of the IEEE/RSJ International Conference on Intelligent Robots and Systems (IROS)*, pages 598–603, Yokohama, Japan.

Han, J., Shao, L., Xu, D., and Shotton, J. (2013). Enhanced computer vision with Microsoft Kinect sensor: A review. *IEEE Transactions on Cybernetics*, 43(5):1318–1334.

Happold, M., Ollis, M., and Johnson, N. (2006). Enhancing supervised terrain classification with predictive unsupervised learning. In *Proceedings of the Robotics: Science and Systems (RSS)*, Philadelphia, PA, USA.

Hornung, A., Wurm, K., Bennewitz, M., Stachniss, C., and Burgard, W. (2013). OctoMap: An efficient probabilistic 3D mapping framework based on octrees. *Autonomous Robots*, 34(3):189–206. Software available at http://octomap.github.com.

Howard, A., Turmon, M., Matthies, L., Tang, B., Angelova, A., and Mjolsness, E. (2006). Towards learned traversability for robot navigation: From underfoot to the far field. *Journal of Field Robotics*, 23(11-12):1005–1017.

Huang, W., Grudic, G., and Matthies, L. (2009). Editorial. *Journal of Field Robots*, 26(1):1–2.

Iagnemma, K. and Buehler, M. (2006). Editorial for the Journal of Field Robotics - Special issue on the DARPA Grand Challenge. *Journal of Field Robotics*, 23(9):655–656.

Jackel, L. D., Krotkov, E., Perschbacher, M., Pippine, J., and Sullivan, C. (2006). The DARPA LAGR program: Goals, challenges, methodology, and phase I results. *Journal of Field Robotics*, 23(11-12):945–973.

Kalmar Global (2016). Autostrad^{TM}. `http://www.kalmarglobal.com/equipment/straddle-carriers/autostrad`. Accessed: 19.03.2016.

Kelly, A., Stentz, A., Amidi, O., Bode, M., Bradley, D., Diaz-Calderon, A., Happold, M., Herman, H., Mandelbaum, R., Pilarski, T., Rander, P., Thayer, S., Vallidis, N., and Warner, R. (2006). Toward reliable off road autonomous vehicles operating in challenging environments. *The International Journal of Robotics Research*, 25(5-6):449–483.

Kim, D., Oh, S. M., and Rehg, J. (2007). Traversability classification for UGV navigation: a comparison of patch and superpixel representations. In *Proceedings of the IEEE/RSJ International Conference on Intelligent Robots and Systems (IROS)*, pages 3166–3173, San Diego, CA, USA.

Kim, D., Sun, J., Oh, S., Rehg, J., and Bobick, A. (2006). Traversability classification using unsupervised on-line visual learning for outdoor robot navigation. In *Proceedings of the IEEE International Conference on Robotics and Automation (ICRA)*, pages 518–525, Orlando, FL, USA.

Kleinehagenbrock, M., Lang, S., Fritsch, J., Lomker, F., Fink, G., and Sagerer, G. (2002). Person tracking with a mobile robot based on multi-modal anchoring. In *Proceedings of the IEEE International Workshop on Robot and Human Interactive Communication*, pages 423–429, Berlin, Germany.

Kluge, B., Kohler, C., and Prassler, E. (2001). Fast and robust tracking of multiple moving objects with a laser range finder. In *Proceedings of the IEEE International Conference on Robotics and Automation (ICRA)*, volume 2, pages 1683–1688, Seoul, Korea.

Kobilarov, M., Sukhatme, G., Hyams, J., and Batavia, P. (2006). People tracking and following with mobile robot using an omnidirectional camera and a laser. In *Proceedings of the IEEE International Conference on Robotics and Automation (ICRA)*, pages 557–562, Orlando, FL, USA.

Krotkov, E., Fish, S., Jackel, L., McBride, B., Perschbacher, M., and Pippine, J. (2007). The DARPA PerceptOR evaluation experiments. *Autonomous Robots*, 22(1):19–35.

Lacaze, A., Murphy, K., and DelGiorno, M. (2002). Autonomous mobility for the Demo III experimental unmanned vehicles. In *Proceedings of the International Conference on Unmanned Systems (AUVSI)*, pages 640–643, Lake Buena Vista, FL, USA.

Lalonde, J., Vandapel, N., Huber, D. F., and Hebert, M. (2006). Natural terrain classification using three-dimensional ladar data for ground robot mobility. *Journal of Field Robotics*, 23(10):839–861.

Lang, T., Plagemann, C., and Burgard, W. (2007). Adaptive non-stationary kernel regression for terrain modelling. In *Proceedings of the Robotics: Science and Systems Conference (RSS)*, Seattle, WA, USA.

LeCun, Y., Bengio, Y., and Hinton, G. (2015). Deep learning. *Nature*, 521:436–444.

Lee, J., Tsubouchi, T., Yamamoto, K., and Egawa, S. (2006). People tracking using a robot in motion with laser range finder. In *Proceedings of the IEEE/RSJ International Conference on Intelligent Robots and Systems (IROS)*, pages 2936–2942, Beijing, China.

Leigh, A., Pineau, J., Olmedo, N., and Zhang, H. (2015). Person tracking and following with 2D laser scanners. In *Proceedings of the International Conference on Robotics and Automation (ICRA)*, pages 726–733, Seattle, WA, USA.

Leighty, R. D. (1986). DARPA ALV (Autonomous Land Vehicle) Summary. Technical Report ADA167472, Army Engineering Topographic Labs, Fort Belvoir, VA.

Leonard, J., How, J., Teller, S., Berger, M., Campbell, S., Fiore, G., Fletcher, L., Frazzoli, E., Huang, A., Karaman, S., Koch, O., Kuwata, Y., Moore, D., Olson, E., Peters, S., Teo, J., Truax, R., Walter, M., Barrett, D., Epstein, A., Maheloni, K., Moyer, K., Jones, T., Buckley, R., Antone, M., Galejs, R., Krishnamurthy, S., and Williams, J. (2008). A perception-driven autonomous urban vehicle. *Journal of Field Robotics*, 25(10):727–774.

Leppänen, I. (2007). *Automatic locomotion mode control of wheel-legged robots*. PhD thesis, Helsinki University of Technology, Espoo, Finland.

Liu, X. (2008). Airborne LiDAR for DEM generation: some critical issues. *Progress in Physical Geography*, 32(1):31–49.

Luber, M., Arras, K., Plagemann, C., and Burgard, W. (2009). Classifying dynamic objects. *Autonomous Robots*, 26(2-3):141–151.

Macedo, J., Manduchi, R., and Matthies, L. (2000). Laser-based discrimination of grass from obstacles for autonomous navigation. In *Proceedings of the International Symposium on Experimental Robotics*, pages 111–120, Honolulu, HI, USA.

Magnusson, M. (2009). *The three-dimensional normal-distributions transform: an efficient representation for registration, surface analysis, and loop detection*. PhD thesis, Laboratory of Applied Autonomous Sensor Systems (AASS), Örebro University, Sweden.

Markoff, J. (2010). Google cars drive themselves, in traffic. *The New York Times*. 9 October.

Martin, S., Murphy, L., and Corke, P. (2013). Building large scale traversability maps using vehicle experience. In Desai, J., Dudek, G., Khatib, O., and Kumar, V., editors, *Experimental Robotics*, volume 88 of *Springer Tracts in Advanced Robotics*, pages 891–905. Springer International Publishing.

Martínez-Barberá, H. and Herrero-Pérez, D. (2010). Autonomous navigation of an automated guided vehicle in industrial environments. *Robotics and Computer-Integrated Manufacturing*, 26(4):296–311.

McHugh, D. (2016). Different paths could lead to autonomous cars. *Associated Press*.

Milch, S. and Behrens, M. (2001). Pedestrian detection with radar and computer vision. In *Proceedings of the Conference on Progress in Automobile Lighting*, Darmstadt, Germany.

Miller, I., Campbell, M., Huttenlocher, D., Kline, F.-R., Nathan, A., Lupashin, S., Catlin, J., Schimpf, B., Moran, P., Zych, N., Garcia, E., Kurdziel, M., and Fujishima, H. (2008). Team Cornell's Skynet: Robust perception and planning in an urban environment. *Journal of Field Robotics*, 25(8):493–527.

Mobileye (2016). Mobileye 5-series. `http://www.mobileye.com/products/mobileye-5-series/`. Accessed: 05.03.2016.

Molino, V., Madhavan, R., Messina, E., Downs, A., Balakirsky, S., and Jacoff, A. (2007). Traversability metrics for rough terrain applied to repeatable test methods. In *Proceedings IEEE/RSJ International Conference on Robotics and Automation (IROS)*, pages 1787–1794, San Diego, CA, USA.

Montemerlo, M., Becker, J., Bhat, S., Dahlkamp, H., Dolgov, D., Ettinger, S., Haehnel, D., Hilden, T., Hoffmann, G., Huhnke, B., Johnston, D., Klumpp, S., Langer, D., Levandowski, A., Levinson, J., Marcil, J., Orenstein, D., Paefgen, J., Penny, I., Petrovskaya, A., Pflueger, M., Stanek, G., Stavens, D., Vogt, A., and Thrun, S. (2008). Junior: The Stanford entry in the Urban Challenge. *Journal of Field Robotics*, 25(9):569–597.

Moravec, H. and Elfes, A. (1985). High resolution maps from wide angle sonar. In *Proceedings of the IEEE International Conference on Robotics and Automation (ICRA)*, volume 2, pages 116–121, Nagoya, Japan.

Mucientes, M. and Burgard, W. (2006). Multiple hypothesis tracking of clusters of people. In *Proceedings of the IEEE/RSJ International Conference on Intelligent Robots and Systems (IROS)*, pages 692–697, Beijing, China.

Myneni, R. and Hall, F. (1995). The interpretation of spectral vegetation indexes. *IEEE Transactions on Geoscience and Remote Sensing*, 33(2):481–486.

Nakane, T. and Soshi, K. (1998). A study on recognition of pedestrians using dual band radar. In *Proceedings of the Intelligent Transport Systems (ITS) World Conference*, Seoul, South Korea.

Nakane, T. and Soshi, K. (2000). Animal body detection system utilizing electromagnetic waves. US Patent 6072173.

NASA (2016). Mars Science Laboratory - Curiosity | NASA. https://www.nasa.gov/mission_pages/msl/index.html. Accessed: 11.02.2016.

National Robotics Engineering Center (2016). Off-Road Autonomy (UPI). http://www.nrec.ri.cmu.edu/projects/upi/index.php. Accessed: 06.03.2016.

Navarro-Serment, L., Mertz, C., and Hebert, M. (2010). Pedestrian detection and tracking using three-dimensional LADAR data. In Howard, A., Iagnemma, K., and Kelly, A., editors, *Field and Service Robotics*, volume 29 of *Springer Tracts in Advanced Robotics*, pages 103–112. Springer Berlin Heidelberg.

Nguyen, D.-V., Kuhnert, L., and Kuhnert, K. (2012a). Spreading algorithm for efficient vegetation detection in cluttered outdoor environments. *Robotics and Autonomous Systems*, 60(12):1498–1507.

Nguyen, D.-V., Kuhnert, L., Thamke, S., Schlemper, J., and Kuhnert, K.-D. (2012b). A novel approach for a double-check of passable vegetation detection in autonomous ground vehicles. In *Proceedings of the International IEEE Conference on Intelligent Transportation Systems (ITSC)*, pages 230–236, Anchorage, AK, USA.

Nieminen, T. and Sampo, M. (1993). Unmanned vehicles for agricultural and off-highway applications. *SAE Technical Paper 932475*.

Nikkei (2016). Japan to develop 3-D maps for self-driving cars. Nikkei Asian Review. 5 September.

nuTonomy (2016). nuTonomy Launches World's First Public Trial of Self-Driving Car Service and Ride-Hailing App. Press release. 25 August.

NVIDIA (2016). Automotive technology solutions overview | NVIDIA. http://www.nvidia.com/object/drive-automotive-technology.html. Accessed: 05.03.2016.

Otero, M. (2000). Application of a continuous wave radar for human gait recognition. In Kadar, I., editor, *Proceedings of the SPIE Signal Processing, Sensor Fusion, and Target Recognition XIV*, volume 5809, Orlando, FL, USA.

Papadakis, P. (2013). Terrain traversability analysis methods for unmanned ground vehicles: A survey. *Engineering Applications of Artificial Intelligence*, 26(4):1373–1385.

Park, H.-W., Wensing, P., and Kim, S. (2015). Online planning for autonomous running jumps over obstacles in high-speed quadrupeds. In *Proceedings of Robotics: Science and Systems (RSS)*, Rome, Italy.

Pejic, I. (2016). Military analysis: U.S. UAV's UGV's, autonomous weapon systems and military robotics. *South Front: Analysis and Intelligence*. 2 February.

Pomerleau, D. (1989). ALVINN: an autonomous land vehicle in a neural network. In Touretzky, D., editor, *Proceedings of the Advances in Neural Information Processing Systems*, volume 1, pages 305–313. Morgan Kaufmann.

Pomerleau, D. and Jochem, T. (1996). Rapidly adapting machine vision for automated vehicle steering. *IEEE Expert*, 11(2):19–27.

Premebida, C., Carreira, J., Batista, J., and Nunes, U. (2014). Pedestrian detection combining rgb and dense lidar data. In *Proceedings of the IEEE/RSJ International Conference on Intelligent Robots and Systems (IROS)*, pages 4112–4117, Chicago, IL, USA.

Prokhorov, D. (2009). Object recignition in 3D LIDAR data with recurrent neural network. In *Proceedings of the IEEE Conference on Computer Society, Computer Vision and Pattern Recognition Workshops*, pages 9–15, Miami, FL, USA.

Raibert, M., Blankespoor, K., Nelson, G., Playter, R., and the BigDog Team (2008). BigDog, the rough-terrain quadruped robot. In *Proceedings of the 17th IFAC World Congress*, Seoul, South Korea.

Rintanen, K., Mäkelä, H., Koskinen, K., Puputti, J., Sampo, M., and Ojala, M. (1996). Development of an autonomous navigation system for an autonomous vehicle. *Control Engineering Practice*, 4(4):499–505.

RoboCup (2016). RoboCup. `http://www.robocup.org/`. Accessed: 06.03.2016.

RoboCup Rescue (2016). RoboCup Rescue Home. `http://www.robocuprescue.org/`. Accessed: 06.03.2016.

Robotics Institute (2012). Robotics Institute: Navlab. `https://www.ri.cmu.edu/research_lab_group_detail.html?lab_id=28&menu_id=263`. Accessed: 19.03.2016.

Rusu, R. B., Sundaresan, A., Morisset, B., Hauser, K., Agrawal, M., Latombe, J.-C., and Beetz, M. (2009). Leaving flatland: Efficient real-time three-dimensional perception and motion planning. *Journal of Field Robotics*, 26(10):841–862.

Saarinen, J., Andreasson, H., Stoyanov, T., and Lilienthal, A. (2013). 3d normal distributions transform occupancy maps: An efficient representation for mapping in dynamic environments. *International Journal of Robotic Research*, 32(14):1627–1644.

Sandvik (2016). Mine automation systems. `http://mining.sandvik.com/en/products/equipment/mine-automation-systems`. Accessed: 05.03.2016.

Santamaria-Navarro, A., Teniente, E., Morta, M., and Andrade-Cetto, J. (2015). Terrain classification in complex three-dimensional outdoor environments. *Journal of Field Robotics*, 32(1):42–60.

Scheutz, M., McRaven, J., and Cserey, G. (2004). Fast, reliable, adaptive, bimodal people tracking for indoor environments. In *Proceedings of the IEEE/RSJ International Conference on Intelligent Robots and Systems (IROS)*, volume 2, pages 1347–1352, Sendai, Japan.

Schiele, B., Andriluka, M., Majer, N., Roth, S., and Wojek, C. (2009). Visual people detection - different models, comparison and discussion. In *Proceedings of the IEEE International Conference on Robotics and Automation (ICRA), Workshop on People Detection and Tracking*, Kobe, Japan.

Schölkopf, B., Platt, J., Shawe-Taylor, J., Smola, A., and Williamson, R. (2001). Estimating the support of a high-dimensional distribution. *Neural Computation*, 13(7):1443–1471.

Schreuder, D. A. (1991). Visibility aspects of the driving task: foresight in driving. Technical Report R-91-71, SWOV Institute for Road Safety Research, Leidschendam, Netherlands.

Schulz, D., Burgard, W., Fox, D., and Cremers, A. (2003). People tracking with mobile robots using sample-based joint probabilistic data association filters. *The International Journal of Robotics Research*, 22(2):99–116.

Sheridan, T. B. (1992). *Telerobotics, Automation, and Human Supervisory Control*. The MIT press, Cambridge, MA, USA.

Sheridan, T. B. (1993). Space teleoperation through time delay: Review and prognosis. *IEEE Transactions on Robotics and Automation*, 9(5):592–606.

Shneier, M., Chang, T., Hong, T., Shackleford, W., Bostelman, R., and Albus, J. (2008). Learning traversability models for autonomous mobile vehicles. *Autonomous Robot*, 24(1):69–86.

Siciliano, B. and Khatib, O., editors (2008). *Springer Handbook of Robotics*. Springer.

Spice, B., Walters, K., and Carvell, K. (2015). Uber, Carnegie Mellon annouce strategic partnership and creation of advanced technologies center in Pittsburg. *Carnegie Mellon University News*. 2 February.

Spinello, L. and Arras, K. (2011). People detection in RGB-D data. In *Proceedings of the IEEE/RSJ International Conference on Intelligent Robots and Systems (IROS)*, pages 3838–3843, San Francisco, CA, USA.

Spinello, L., Arras, K., Triebel, R., and Siegwart, R. (2010). A layered approach to people detection in 3D range data. In *Proceedings of the AAAI Conference on Artificial Intelligence, Physically Grounded AI Track*, Atlanta, GA, USA.

Stoyanov, T., Magnusson, M., Andreasson, H., and Lilienthal, A. (2010). Path planning in 3D environments using normal distributions transform. In *Proceedings of the IEEE/RSJ International Conference on Intelligent Robots and Systems (IROS)*, pages 3263–3268, Taipei, Taiwan.

Stoyanov, T., Magnusson, M., and Lilienthal, A. (2013). Comparative evaluation of the consistency of three-dimensional spatial representation used in autonomous robot navigation. *Journal of Field Robotics*, 30(2):216–236.

Suomela, J. (2004). *From teleoperation to the cognitive human-robot interface*. PhD thesis, Helsinki University of Technology, Espoo, Finland.

Thorpe, C., Hebert, M., Kanade, T., and Shafer, S. (1988). Vision and navigation for Carnegie-Mellon Navlab. *IEEE Transactions on Pattern Analysis and Machine Intelligence*, 10(3):362–373.

Thrun, S., Montemerlo, M., Dahlkamp, H., Stavens, D., Aron, A., Diebel, J., Fong, P., Gale, J., Halpenny, M., Hoffmann, G., Lau, K., Oakley, C., Palatucci, M., Pratt, V., Stang, P., Strohband, S., Dupont, C., Jendrossek, L.-E., Koelen, C., Markey, C., Rummel, C., van Niekerk, J., Jensen, E., Alessandrini, P., Bradski, G., Davies, B., Ettinger, S., Kaehler, A., Nefian, A., and Mahoney, P. (2006). Stanley: The robot that won the DARPA grand challenge. *Journal of Field Robotics*, 23(9):661–692.

Time Magazine (1925). Science: Radio Auto. *Time Magazine*. 10 August.

Topp, E. and Christensen, H. (2005). Tracking for following and passing persons. In *Proceedings of the IEEE/RSJ International Conference on Intelligent Robots and Systems (IROS)*, pages 2321–2327, Edmonton, Canada.

Trepagnier, P. G., Nagel, J., Kinney, P. M., Koutsougeras, C., and Dooner, M. (2006). Kat-5: Robust systems for autonomous vehicle navigation in challenging and unknown terrain. *Journal of Field Robotics*, 23(8):509–526.

Triebel, R., Pfaff, P., and Burgard, W. (2006). Multi-level surface maps for outdoor terrain mapping and loop closing. In *Proceedings of the IEEE/RSJ International Conference on Intelligent Robots and Systems (IROS)*, pages 2276–2282, Beijing, China.

Tsugawa, S. (1994). Vision-based vehicles in Japan: Machine vision systems and driving control systems. *IEEE Transactions on Industrial Electronics*, 41(4):398–405.

Uber Newsroom (2016). Steel City's New Wheels. Press release. 19 May.

Urmson, C., Anhalt, J., Bae, H., Bagnell, J., Baker, C., Bittner, R., Brown, T., Clark, M., Darms, M., Demitrish, D., Dolan, J., Duggins, D., Ferguson, D., Galatali, T., Geyer, C., Gittleman, M., Harbaugh, S., Hebert, M., Howard, T., Kolski, S., Likhachev, M., Litkouhi, B., Kelly, A., McNaughton, M., Miller, N., Nickolaou, J., Peterson, K., Pilnick, B., Rajkumar, R., Rybski, P., Sadekar, V., Salesky, B., Seo, Y.-W., Singh, S., Snider, J., Struble, J., Stentz, A., Taylor, M., Whittaker, W., Wolkowicki, Z., Zhang, W., and Ziglar, J. (2008). Autonomous driving in urban environments: Boss and the Urban Challenge. *Journal of Field Robotics*, 25(8):425–466.

Urmson, C., Ragusa, C., Ray, D., Anhalt, J., Bartz, D., Galatali, T., Gutierrez, A., Johnston, J., Harbaugh, S., "Yu" Kato, H., Messner, W., Miller, N., Peterson, K., Smith, B., Snider, J., Spiker, S., Ziglar, J., "Red" Whittaker, W., Clark, M., Koon, P., Mosher, A., and Struble, J. (2006). A robust approach to high-speed navigation for unrehearsed desert terrain. *Journal of Field Robotics*, 23(8):467–508.

Vandapel, N., Huber, D., Kapuria, A., and Hebert, M. (2004). Natural terrain classification using 3-D ladar data. In *Proceedings of the IEEE International Conference on Robotics and Automation (ICRA)*, volume 5, pages 5117–5122, New Orleans, LA, USA.

Vasudevan, S., Ramos, F., Nettleton, E., and Durrant-Whyte, H. (2009). Gaussian process modeling of large-scale terrain. *Journal of Field Robotics*, 26(10):812–840.

Vis, I. F. A. (2006). Survey of research in the design and control of automated guided vehicle systems. *European Journal of Operational Research*, 170(3):677–709.

VisLab (2013). PROUD car test. `http://vislab.it/proud-en/`. Accessed: 19.03.2016.

VisLab (2014). Presentation of DEEVA. `http://vislab.it/events/presentation-of-new-vehicle/`. Accessed: 19.03.2016.

Walter, B. E., Knutzon, J. K., Sannier, A. V., and Oliver, J. H. (2004). Virtual UAV ground control station. In *Proceedings of the AIAA "Unmanned Unlimited" Technical Conference, Workshop, and Exhibit*, Chicago, IL, USA.

Wellington, C. (2005). *Learning a Terrain Model for Autonomous Navigation in Rough Terrain*. PhD thesis, Robotics Institute, Carnegie Mellon University, PA, USA.

Wellington, C., Courville, A., and Stentz, A. (2006). A generative model of terrain for autonomous navigation in vegetation. *The International Journal of Robotics Research*, 25(12):1287–1304.

Wellington, C. and Stentz, A. (2004). Online adaptive rough-terrain navigation vegetation. In *Proceedings of the IEEE International Conference on Robotics and Automation (ICRA)*, volume 1, pages 96–101, New Orleans, LA, USA.

Wiemann, T., Nuchter, A., Lingemann, K., Stiene, S., and Hertzberg, J. (2010). Automatic construction of polygonal maps from point cloud data. In *Proceedings of the IEEE International Workshop on Safety Security and Rescue Robotics (SSRR)*, Bremen, Germany.

Woof, M. (2005). Technology for underground loading and hauling systems offers exciting prospects. *Engineering and Mining Journal*, 206(3):32–34,38.

Wurm, K., Kretzschmar, H., Kümmerle, R., Stachniss, C., and Burgard, W. (2014). Identifying vegetation from laser data in structured outdoor environments. *Robotics and Autonomous Systems*, 62(5):675–684.

Xia, L., Chen, C.-C., and Aggarwal, J. K. (2011). Human detection using depth information by Kinect. In *Proceedings of the IEEE Conference on Computer Society, Computer Vision and Pattern Recognition Workshops*, pages 15–22, Colorado Springs, CO, USA.

Xin, L. and Bin, D. (2013). The latest status and development trends of military unmanned ground vehicles. In *Proceedings of the Chinese Automation Congress*, pages 533–537, Changsha, China.

Yarovoy, A., Ligthart, L., Matuzas, J., and Levitas, B. (2008). UWB radar for human being detection. *IEEE Aerospace and Electronic Systems Magazine*, 23(5):36–40.

Ye, C. and Borenstein, J. (2004). T-transformation: a new traversability analysis method for terrain navigation. In Gerhart, G., Gage, D., and Shoemaker, C., editors, *Proceedings of the SPIE: Unmanned Ground Vehicle Technology VI*, volume 5422, pages 473–483, Orlando, FL, USA.

Ylönen, S. (2006). *Modularity in service robotics — Techno-economic justification through a case study*. PhD thesis, Helsinki University of Technology, Espoo, Finland.

Zhou, S., Xi, J., McDaniel, M., Nishihata, T., Salesses, P., and Iagnemma, K. (2012). Self-supervised learning to visually detect terrain surfaces for autonomous robots operating in forested terrain. *Journal of Field Robotics*, 29(2):277–297.

Aalto-DD 175/2017

ISBN 978-952-60-7613-3 (printed)
ISBN 978-952-60-7612-6 (pdf)
ISSN-L 1799-4934
ISSN 1799-4934 (printed)
ISSN 1799-4942 (pdf)

Aalto University
School of Electrical Engineering
Department of Electrical Engineering and Automation
www.aalto.fi

BUSINESS +
ECONOMY

ART +
DESIGN +
ARCHITECTURE

SCIENCE +
TECHNOLOGY

CROSSOVER

DOCTORAL
DISSERTATIONS